Assessing the constraints on the accuracy of SWOT satellite water detection in wetlands

A thesis submitted in partial fulfillment of the requirements for
the degree of Bachelor of Environment and Sustainability Advanced (Honours)

by

Maya Taib

Supervisor:
Prof. Paul Tregoning

Earth and Marine Science
Research School of Earth Sciences
The Australian National University

21 October 2026



Australian
National
University

Declaration

This thesis is an account of research undertaken between February 2026 and October 2026 at The Research School of Earth Sciences, The Australian National University, Canberra, Australia.

Except where acknowledged in the customary manner, the material presented in this thesis is, to the best of my knowledge, original and has not been submitted in whole or part for a degree in any university.

Maya Taib
21 October 2026

Acknowledgements

I would first like to thank my supervisor, Professor Paul Tregoning. I am very grateful to have had such a supportive supervisor who has helped build my confidence in doing research over the past year. Thank you for all your help and advice, and for encouraging me to keep questioning and learning things.

Thanks to the whole Environmental Geodesy group for the invaluable input throughout my project and for our fun lunchtime conversations! Thanks also to everyone I've met at RSES this year for making me feel welcome.

Finally, thank you to my family and friends for your support and encouragement, as always.

This work was completed with financial support from an A L Hales Honours Year Scholarship and an Australian Computer Society Foundation Women of STEM Scholarship.

Abstract

Wetlands are critical ecosystems that provide important ecological, socio-cultural and economic services. However, wetlands globally are increasingly threatened by changing hydrological regimes due to climate change and intensifying human demands for water. In the face of these pressures, it is critical to monitor the quantity, frequency and spatial extent of water flows within wetlands, in order to better understand long-term changes in wetland health, and to guide management actions to protect and restore these ecosystems. However, wetlands are highly complex and dynamic landscapes that are challenging to monitor consistently and at a global scale. Currently, various in situ and remote sensing techniques have been used to monitor wetland hydrology. While in situ methods provide accurate measurements of water extent, discharge, depth and quality, they are expensive and spatially limited. Similarly, airborne remote sensing has limited spatial and temporal coverage. Satellite remote sensing offers a cheaper and larger scale monitoring method, but current satellite missions are limited by their individual instrumental capabilities. In particular, there has been no consistent method of directly measuring water surface elevations across wetlands lacking in situ measurements. The new Surface Water and Ocean Topography (SWOT) satellite mission offers this capability, using Ka-band radar interferometry to measure the water extents and water surface elevations across inland water bodies at a spatial resolution of ∼10-60 m, every 21 days. However, the ability of SWOT to detect water under the complex surface conditions found within wetlands remains uncertain.

In this thesis, I first assessed SWOT water detection in a natural Australian wetland system by comparing SWOT-derived water extents with independent optical satellite observations. I identified several cases where SWOT failed to detect water surfaces. To investigate this issue, I assessed SWOT water detection in a controlled test case of several large, vegetated farm dams in southern Queensland. I first developed a fill model using land topography data and SWOT water surface elevation estimates to simulate the water extents and depths across the dams. I compared these modelled extents to independent optical satellite-derived water extents and to SWOT water extents. I found cases where SWOT misclassified wet soil as water, suggesting that the SWOT processing algorithm may be overly sensitive to soil moisture. I also found cases where SWOT misclassified water areas as land, which sometimes correlated with increased height of emergent vegetation above the water surface. However, this correlation was inconsistent, suggesting that the impact of emergent vegetation on the accuracy of SWOT water detection is complex and likely influenced by other surface characteristics such as vegetation density and wind. The constraints I identified on the accuracy of SWOT water detection will be important considerations for end-users utilising SWOT observations to quantify water extent and

volume within wetlands.

Despite these constraints, SWOT offers complementary capabilities to current wetland monitoring techniques. It provides important, new observations that can be used in combination with existing remote sensing and modelling methods to aid with the monitoring and management of wetlands globally.

Contents

Declaration ii

Acknowledgements iii

Abstract iv

1 Introduction 1
- 1.1 Water availability and wetland conservation . . . 1
- 1.2 Importance of water for wetland functioning . . . 2
- 1.3 Monitoring of wetland hydrology . . . 2
  - 1.3.1 Importance of wetland monitoring . . . 2
  - 1.3.2 Monitoring tools . . . 3
  - 1.3.3 Surface Water and Ocean Topography (SWOT) satellite . . . 4
- 1.4 Objectives of this thesis . . . 5

2 Literature review 6
- 2.1 Challenges of wetland monitoring using remote sensing . . . 6
- 2.2 Airborne LiDAR . . . 7
- 2.3 Satellite systems . . . 10
  - 2.3.1 Sentinel-2 . . . 10
  - 2.3.2 SWOT . . . 14

3 Constraints on the accuracy of SWOT water detection in wetlands 19
- 3.1 Introduction . . . 20
- 3.2 Data . . . 23
  - 3.2.1 Study site . . . 23
  - 3.2.2 Dam bathymetry . . . 23
  - 3.2.3 SWOT water detection . . . 23
  - 3.2.4 Simulated water extent . . . 24
  - 3.2.5 Sentinel-2 water extent . . . 24
  - 3.2.6 Vegetation cover . . . 25
- 3.3 Comparison of fill model water extents with Sentinel-2 water extents . . . 25
- 3.4 SWOT detection of shallow water and wet soil . . . 26
- 3.5 Impact of vegetation on SWOT water detection . . . 26
- 3.6 Discussion . . . 31
- 3.7 Conclusion . . . 32

4 Supporting information for manuscript **34**
4.1 Sentinel-2 data and Modified Normalised Difference Water Index (MNDWI) 34
4.2 Description of the Tasseled Cap Wetness (TCW) index 35
4.3 Similarity assessment of fill model water extents and Sentinel-2 water extents 35
4.4 Plotting of DEM and canopy height raster transects and SWOT pixel transects 36
4.5 Rasterisation of SWOT pixels 37

5 Discussion and conclusions **40**
5.1 Limitations of this study 40
5.1.1 Datasets 40
5.1.2 Raster-based analysis 40
5.2 Improving the SWOT PIXC data product 41
5.3 Implications for wetland monitoring 42
5.3.1 Improving SWOT water extent retrievals 42
5.3.2 Implications for SWOT water surface elevation retrievals 43
5.4 Conclusions 43

References **45**

List of Figures

1.1 Schematic diagram of SWOT satellite 4

2.1 1 m Digital Elevation Model of a Cubbie Station dam 7
2.2 5 m Digital Elevation Model of the Narran Lakes wetland 9
2.3 Water extents across the Narran Lakes wetland using the MNDWI and TCW index with different thresholds 12
2.4 Clear and cloud-covered Sentinel-2 image 13
2.5 Incidence angles of SWOT PIXC pixels 17

3.1 Narran Lakes wetland water extent from Sentinel-2 and SWOT 22
3.2 SWOT detection of soil moisture 27
3.3 SWOT water detection accuracy under different canopy heights 28
3.4 SWOT water detection compared to coherent power and canopy height . . 30

4.1 Cubbie Station study site map 37
4.2 Similarity between MNDWI and fill model water extents 38
4.3 Similarity between TCW index and fill model water extents 39

Chapter 1

Introduction

1.1 Water availability and wetland conservation

Water is a fundamental resource for life on Earth. However, global water availability is increasingly threatened by intensifying human demands and a changing climate (Falkenmark et al., 2019; Chandanpurkar et al., 2025). The world has shifted into a state of 'water bankruptcy' in which the water use in many regions has exceeded a renewable limit (Madani, 2026). By 2050, almost half of the world's nations are predicted to experience water scarcity (Baggio et al., 2021), which will increasingly cause profound and irreversible impacts on the health and survival of humans and the natural environment (Matta et al., 2026). Freshwater ecosystems are particularly vulnerable to changing water availability, with many surviving in a fine balance between their ecological needs and the water resources available to support them (Sayer et al., 2025; Bunn & Arthington, 2002). Globally, wetlands provide up to $39 trillion in benefits to society (Robertson et al., 2025) by supplying food, regulating our climate, supporting rich biodiversity, and providing social and cultural value to communities. Therefore, the continuing degradation of these vulnerable environments severely threatens the ecosystem services they provide (Lynch et al., 2023).

In Australia, the distribution of water resources is highly variable, due to natural climate variability over space and time (D. L. Liu et al., 2021). Past and current river regulation has aimed to harness water flows for human use, resulting in modified hydrological regimes across much of south-eastern Australia (Leblanc et al., 2021). These changes have caused reductions in the water flows into many of Australia's floodplain wetlands, leading to the degradation of these vulnerable, highly specialised ecosystems (Kingsford, 2000; Chen et al., 2020; Kreibich et al., 2024). Australia's wetlands support nationally and internationally significant biodiversity (Bino et al., 2014), provide deep cultural value to Indigenous peoples (Marshall, 2017), and offer important social and recreational value to local communities and tourists (Smart et al., 2026; Streever et al., 1998). These values therefore depend on the protection and restoration of Australia's wetlands.

To address the serious threats to freshwater ecosystems, global political mobilisation has established goals for the conservation and restoration of wetland environments. For instance, the Ramsar Convention is an intergovernmental treaty that provides a framework for the conservation and wise use of wetlands (*Convention on Wetlands of International Importance especially as Waterfowl Habitat*, 1971). Party states designate 'Wetlands of International Importance' and are obliged to conserve the ecological character of these

sites. This includes maintaining the "ecosystem components, processes, benefits and services that characterise the wetland" (Ramsar Convention, Resolution IX.1 Annex A). As a party to the Ramsar Convention, the Australian Government has committed to protecting its 67 Ramsar sites. In order to uphold this commitment, suitable hydrological conditions must be maintained to conserve the ecological character of these wetlands (Department of the Environment and Energy, 2015).

1.2 Importance of water for wetland functioning

Wetland functioning depends on complex interactions between water, soils, and biological and geochemical processes (Jackson et al., 2014). The key hydrological parameters driving these interactions are water surface elevation, extent, depth, timing, and flow patterns. These parameters influence geobiochemical processes such as nutrient and carbon cycling, as well as the composition, richness and abundance of wetland-dependent flora and fauna (Bunn & Arthington, 2002; Mason et al., 2022). For example, the occurrence, timing and success of waterbird breeding events across wetlands in Australia's Murray-Darling Basin are predominantly driven by the timing, duration and depths of inundation events (Brandis et al., 2011; Arthur et al., 2012; Bino et al., 2014; Rogers, 2011). Similarly, wetland-dependent vegetation communities require frequent inundation over a sufficiently large area in order to survive (Department of Climate Change, Energy the Environment and Water, 2025).

1.3 Monitoring of wetland hydrology

1.3.1 Importance of wetland monitoring

Monitoring wetland hydrology is critical for understanding the impacts of natural and human-induced hydrological regime variability on the health and functioning of wetland ecosystems. Detailed and frequent monitoring of water flows and depths upstream of and within wetlands helps wetland managers track potential long-term changes in water availability across important wetlands. These insights help monitor and predict associated shifts in wetland condition, guiding management interventions such as ecological restoration or, in regulated river systems like the Murray-Darling Basin, the release of environmental water to support specific wetland ecological processes (e.g. Goulburn-Broken Catchment Management Authority (2024)). State and federal government research programs such as the NSW Rivers Environmental Restoration Program have highlighted the importance of robust wetland monitoring to "inform adaptive management and justify government investment in wetland health" (Department of Environment, Climate Change and Water NSW, 2011).

More broadly, the monitoring of wetland hydrology is important for informing regional water resources management. Wetlands are a key component in the hydrological cycle, influencing surface water storage and flows (Bullock & Acreman, 2003). Quantifying

these contributions is therefore important for catchment managers to model the water resources available for ecological and consumptive uses within a catchment (e.g. Rayburg and Thoms (2009)). This is particularly critical for predicting the impacts of climate change and hydrological variability on regional water availability. Importantly, one of the key requirements for hydrodynamic and hydrological modelling is the use of accurate calibration and validation data from the system being modelled (Van Dijk & Renzullo, 2011). This includes information on wetland hydrology such as inundation dynamics and flows between river channels and wetlands (Makungu & Hughes, 2021).

1.3.2 Monitoring tools

A range of monitoring tools provide multi-scale insights into wetland hydrology. In situ methods such as river gauges provide direct, sub-hourly measurements of water level, discharge, and quality. However, these yield only point-scale data, and many wetlands are remote and may have only few in situ gauges, or none at all. The availability of accurate hydrological information in these vulnerable ecosystems is therefore limited. Relying on few in situ measurements is insufficient for obtaining the breadth of information required for managing complex wetland environments (Gilvear & Bradley, 2000).

On the other hand, airborne and satellite remote sensing systems enable comparatively inexpensive and regional or global monitoring (Guo et al., 2017). Airborne systems can observe wetland water features in high spatial detail (Anokye & Hashemi-Beni, 2026), and can map landscape topography to enable the estimation of floodwater depths (Penton et al., 2023) and the modelling of water flows (Thoms et al., 2007). However, airborne systems are resource-intensive to operate and have relatively limited spatial and temporal coverage.

Satellite systems provide accessible, frequent and scalable observations across the world's wetlands (Guo et al., 2017). Different sensors have mixed capabilities for monitoring hydrological parameters across a variety of spatial and temporal scales. Optical sensors that passively detect sunlight reflected from the Earth's surface can directly estimate wetland water extent (Pekel et al., 2016; Lehner et al., 2025) and water quality (Hou et al., 2022). However, these systems are ineffective in cloudy conditions, limiting their applicability in many regions of the world. On the other hand, active satellite remote sensing systems like Synthetic Aperture Radar (SAR) satellites that send pulses of radar energy to the Earth's surface and detect its return are capable of all-weather monitoring. This makes them useful for detecting wetland water extents globally (Musa et al., 2015).

However, neither optical nor SAR systems are capable of directly measuring water surface elevation, a key hydrological parameter in inland water bodies. Water surface elevation is defined as the height of a water surface above a reference surface (e.g. a reference ellipsoid model of the Earth), and is equivalent to the sum of the land topography and the water depth.

1.3.3 Surface Water and Ocean Topography (SWOT) satellite

The Surface Water and Ocean Topography (SWOT) satellite mission, launched in December 2022, offers unprecedented capabilities for hydrological monitoring compared to existing satellite sensors (Biancamaria et al., 2016) (Figure 1.1). SWOT uses interferometric SAR (i.e. a technique that compares two SAR images captured simultaneously) to estimate the water surface elevation across inland water bodies with high accuracy, at a spatial resolution of ∼10-60 m and, at minimum, every 21 days. SWOT has been used to quantify water storage and flows within a variety of water bodies, including lakes and reservoirs (Maubant et al., 2025; Girard et al., 2025; Rai et al., 2026b), rivers (Cerbelaud et al., 2026; Hart-Davis et al., 2026), and wetlands (Kica et al., 2025; Callaway et al., 2026; Salameh et al., 2026). The unique ability of SWOT to estimate water surface elevations also allows for the estimation of water depths across these water bodies, provided that accurate land topography data is available (Callaway et al., 2026; Rai et al., 2026b).

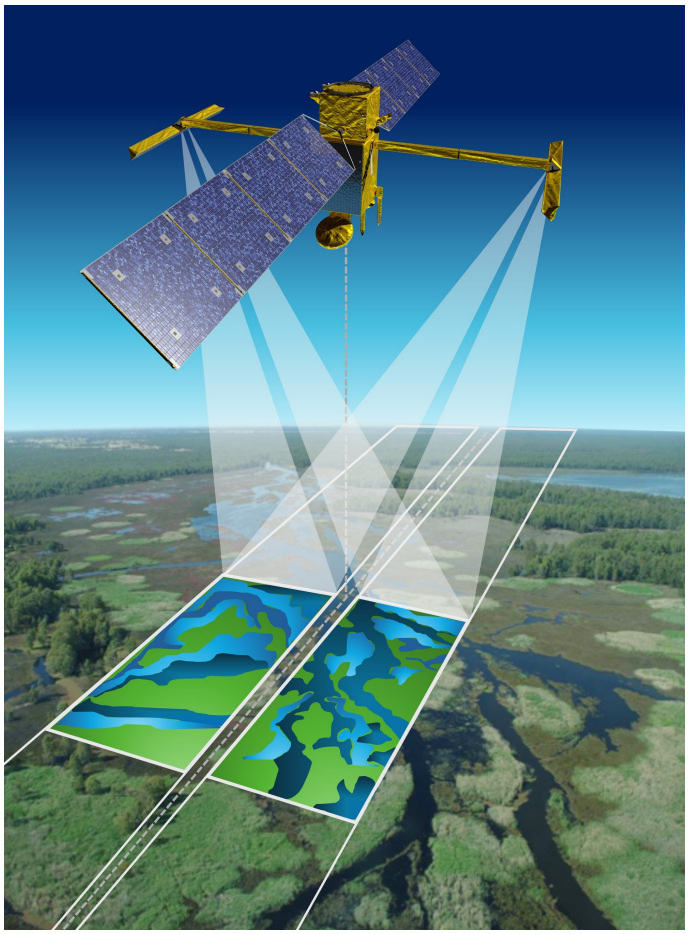


Figure 1.1: Schematic diagram of the SWOT satellite monitoring an Australian wetland (not to scale).

However, the accuracy of SWOT water level observations across water surfaces in complex wetland environments relies on the ability of the sensor to correctly distinguish water areas from land. Current studies investigating this capability are limited, but have

generally found that SWOT water detection may be more challenging when vegetation and soil moisture are present (Desrochers et al., 2021; Kica et al., 2025; Callaway et al., 2026; Bonassies et al., 2026). Given the significant potential that the SWOT mission offers for transforming the monitoring and management of freshwater environments, it is imperative to clarify the potential impacts of land surface characteristics on the utility of SWOT in wetlands globally (Beltrão et al., 2026).

1.4 Objectives of this thesis

This thesis investigates the constraints on the accuracy of SWOT water detection in wetland landscapes. I begin by assessing SWOT water detection in a natural Australian wetland system, the Ramsar-listed Narran Lakes wetland in northern NSW. I compare SWOT water extents with independent optical satellite data, and identify several cases where SWOT incorrectly identifies water-covered areas as land. To investigate this further, I assess the capability of SWOT to detect water in a controlled test case of several large farm dams on Cubbie Station in southern Queensland. My aims are to:

- Identify cases where SWOT correctly detects water-covered areas,
- Identify cases where SWOT incorrectly detects water areas as land or land areas as water,
- Investigate potential reasons for the incorrect SWOT water detections.

Chapter 1 has described the background of the study, including the importance of wetlands and an overview of the tools used to monitor wetland hydrology, including SWOT.
Chapter 2 describes in further detail the remote sensing tools that my study uses, and the current understanding of the capabilities of these systems for water detection in wetlands.
Chapter 3 describes the main study undertaken to assess the accuracy of SWOT water detection in the Cubbie Station farm dams. This chapter has been submitted as a manuscript to *Geophysical Research Letters* (currently under review):
Taib, M. and Tregoning, P., 2026. Constraints on the accuracy of SWOT water detection in wetlands, manuscript submitted to *Geophysical Research Letters* on 7 September 2026.
Chapter 4 presents a discussion of the findings and overall conclusions.

Chapter 2

Literature review

In Chapter 1 I discussed the importance of monitoring wetland hydrology and briefly described the in situ, airborne and satellite methods used. In this chapter, I describe in more detail the remote sensing methods I use in the main study, including how they operate and their strengths and limitations for detecting water in wetlands.

2.1 Challenges of wetland monitoring using remote sensing

Wetlands are highly diverse and heterogeneous landscapes that change dynamically over space and time. This means that monitoring wetlands consistently and efficiently can be challenging (Gallant, 2015). Globally, wetlands cover an area of up to 18 million square kilometres (Lehner et al., 2025). While they are all characterised by the presence of water, there exists significant variation in the surface characteristics present across different wetland types, such as differences in their geomorphology and the ecological communities they support. Furthermore, wetlands are highly dynamic landscapes that respond to changing biophysical conditions (Gilvear & Bradley, 2000). For example, the growth of wetland vegetation responds dynamically following inundation events (M. Liu et al., 2024; Raulings et al., 2010). This means that the surface properties of wetlands that are observable by remote sensing tools can change drastically over space and through time, reducing the consistency and repeatability of observations in these environments. In addition, many wetlands contain steep environmental gradients on spatial scales that are often unresolvable by remote sensing systems. For instance, the boundary between a water and land surface in a wetland may appear as a 'mixed' pixel, complicating water delineation in this zone (Mueller et al., 2016).

These unique characteristics make water detection in wetland environments using remote sensing particularly challenging. Nevertheless, there is a range of available remote sensing tools that operate on different spatial and temporal scales, each with different technical capabilities that help address these challenges. These tools provide valuable hydrological information that would otherwise be unavailable or difficult to obtain using in situ wetland monitoring methods (Guo et al., 2017).

2.2 Airborne LiDAR

Airborne Light Detection and Ranging (LiDAR) systems are commonly used to characterise surface features of wetlands in immense detail (Anokye & Hashemi-Beni, 2026). LiDAR operates by sending pulses of energy to the Earth's surface and measuring their return time, to create a high density point cloud (with 1-20 points/m^2) of the elevations of the land and any surface features (Shan & Toth, 2008). Airbone LiDAR has been used extensively for a variety of applications, including hydrology (Ritchie, 1996), forestry (Hyyppä et al., 2009), archaeology (Vinci et al., 2025), urban design (Yan et al., 2015) and geophysics (Sun et al., 2022). From a LiDAR-derived point cloud, analysts can produce Digital Elevation Models (DEMs), which are gridded representations of the topography of the land (e.g. Figure 2.1). DEMs are critical datasets for the hydrological monitoring of wetlands, as the topography (and the bathymetry) of a wetland dictates the area and depth of inundation (Haag et al., 2005; Penton et al., 2025).

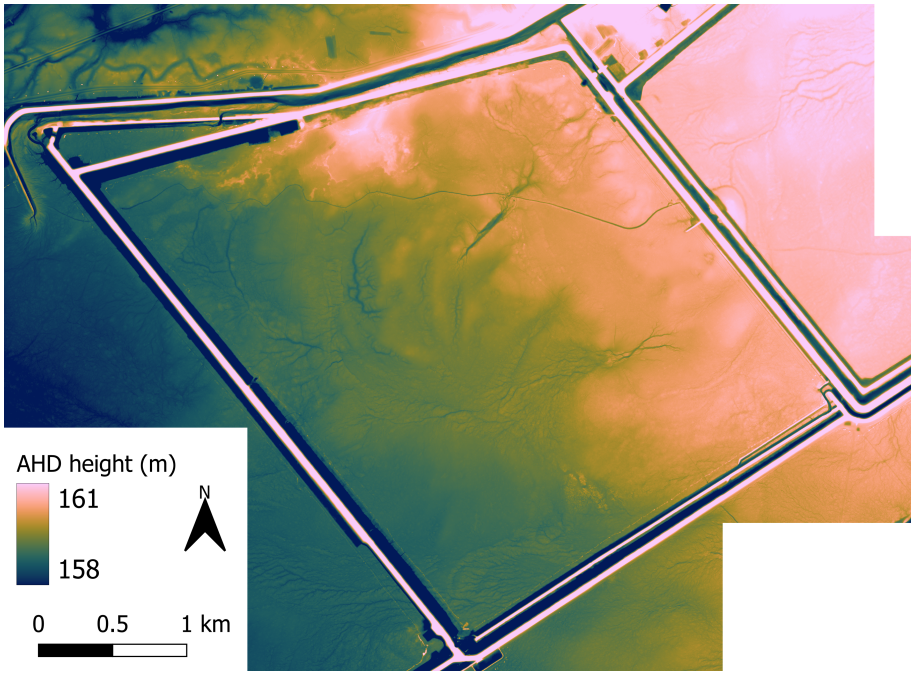


Figure 2.1: Example of a LiDAR-derived 1 m DEM of a Cubbie Station dam, created from publicly available DEM tiles of the region (State of Queensland Department of Natural Resources, Mines and Energy, 2019). Land heights are provided relative to the Australian Height Datum (AHD) relative to the AUSGeoid09.

One of the applications of DEMs in wetland monitoring is to estimate water depths. Prior to the SWOT mission, depth estimation methods relied on the combination of a DEM with water extents obtained from airborne or spaceborne imaging (Teng et al., 2022; Psomiadis et al., 2019). For example, this approach is employed in the Floodwater Depth Estimation Tool (FwDET) developed by Cohen et al. (2018). The FwDET works by first extracting the water surface elevations where the boundaries of the flooded areas

intersect the DEM, and interpolating these over the entire flooded areas. The land elevations are then subtracted from the interpolated water surface elevations to obtain water depth estimates (Cohen et al., 2018). Penton et al. (2023) used the FwDET to produce maps of estimated maximum floodwater depths across the Murray-Darling Basin by combining DEMs of the dry land surface with water extents derived from cloud-free Landsat optical satellite imagery. Since the launch of the SWOT mission, water depths can now be estimated every 11-21 days by subtracting DEM land heights from the water surface elevation estimates obtained by SWOT (Callaway et al., 2026). However, this process depends on obtaining accurate water surface elevation estimates from areas where SWOT correctly identifies water (see Section 2.3.2 for a description of the SWOT water detection process).

The other main application of DEMs in wetland monitoring is for the modelling of water extents and flows (Rayburg & Thoms, 2009; Teng et al., 2017). This can be done through relatively simple conceptual Geographical Information System (GIS) techniques or more complex hydrodynamic modelling. GIS-based approaches typically simulate the extent and/or depth of water in depressions across a landscape at different water levels or with different amounts of water inflow (Shook et al., 2021; Wu & Lane, 2017; Chandler et al., 2024; Townsend & Walsh, 1998). These approaches have been used for informing flood hazard planning (Armstrong et al., 2013) and identifying potential areas within wetlands that are suitable for vulnerable wetland species (Chandler et al., 2024). On the other hand, hydrodynamic models provide more comprehensive predictions of inundation extents, depths and velocities across wetlands and their surrounding floodplains. These models integrate a DEM with equations of water flow, in situ river gauge measurements, inundation maps and biophysical parameters like climatic and terrain characteristics (Teng et al., 2017; De Paiva et al., 2013; Karim et al., 2024). While hydrodynamic models can provide more comprehensive insights into floodplain hydrology, they are complex to develop and computationally intensive to implement (Teng et al., 2017).

Importantly, the utlity of DEMs for water depth estimation and modelling depends on the availability of a DEM of wetland bathymetry, created from a LiDAR survey of the dry land surface or using bathymetric LiDAR that can penetrate the water column (Anokye & Hashemi-Beni, 2026). For example, Figure 2.2 shows a wetland DEM with missing bathymetry measurements due to the presence of water during the LiDAR survey. These gaps would need to be infilled using interpolation, which would decrease the accuracy of water depth estimates or hydrological models derived using this DEM.

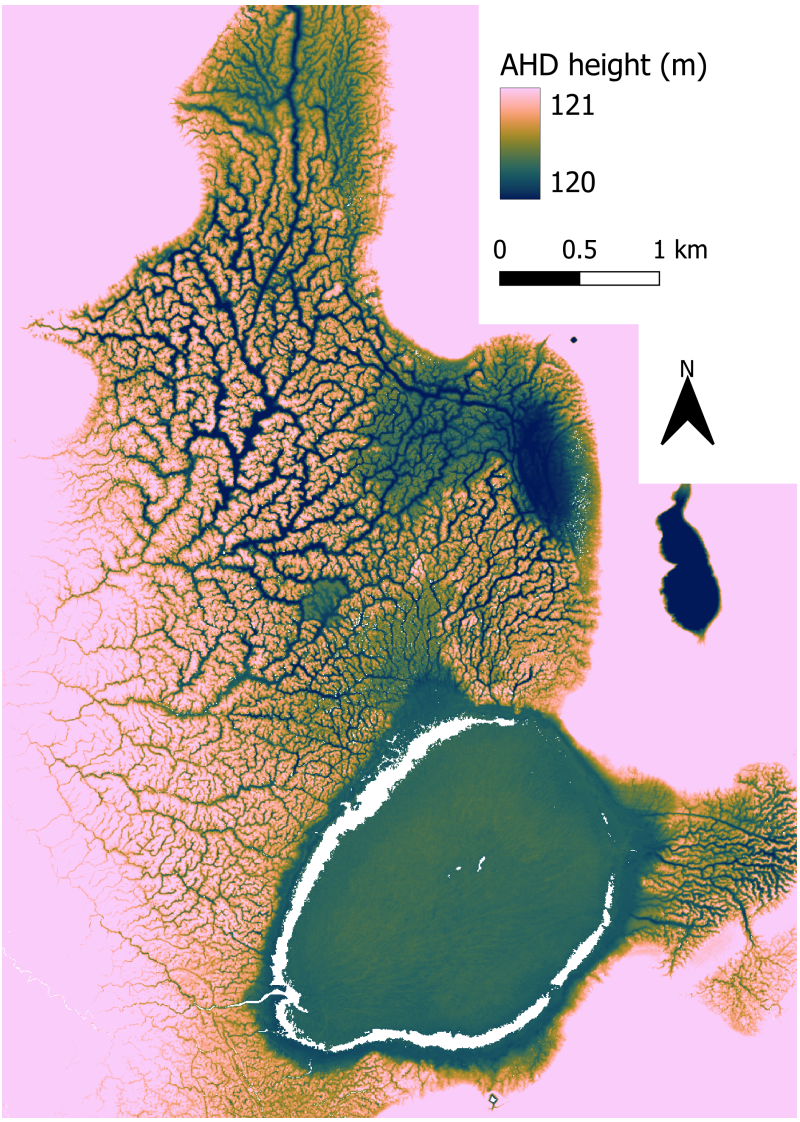


Figure 2.2: LiDAR-derived 5 m DEM of the Narran Lakes wetland, created from publicly available LiDAR point clouds of the region (Spatial Services, NSW Government, 2025). Land heights are provided relative to the Australian Height Datum (AHD) relative to the AUSGeoid09. The white pixels are areas that were covered in water during the LiDAR survey, where bathymetry could not be obtained.

Furthermore, the accuracy of the estimated water extents and depths depends on the spatial resolution and accuracy of the DEMs used (Penton et al., 2023). Generally, the spatial resolution of the DEM (i.e. the size of individual grid cells) is chosen to balance computational efficiency with the ability of the DEM to adequately represent the scale of topographic variability across the landscape (high resolution DEMs are more accurate but require more processing resources) (Wechsler, 2007). Using LiDAR is therefore ideal, as the high density point clouds can be gridded to create a DEM at the desired spatial resolution. Nevertheless, LiDAR-derived DEMs are generally affected by three main sources of error (X. Liu et al., 2015): sensor error (horizontal and vertical error from the LiDAR data

collection), ground error (errors in selecting LiDAR points that represent the ground surface) and interpolation error (errors introduced when gridding LiDAR points). These generally result in DEMs with decimetre-scale horizontal and vertical accuracy.

The fill model I develop in Chapter 3 requires an accurate DEM of the bathymetry of the farm dams. Fortunately, a LiDAR survey was conducted in the region in December 2018 by the Queensland government during a drought period when all the dams were empty (State of Queensland Department of Natural Resources, Mines and Energy, 2019). A pre-processed 1 m Bare Earth DEM derived from this LiDAR survey is publicly available (Figure 2.1), which has a quoted vertical and horizontal accuracy of 0.3 m and 0.8 m, respectively. I use this DEM and a GIS-based fill model to simulate the extent and depths of water across the farm dams, by 'filling' the DEM cells with elevations below the water surface elevation estimates obtained from SWOT (see Section 3.2.4 for a detailed description of this method). While this model is relatively simple, it is adequate for simulating the water extents across the dams, which have relatively uniform topographies and filling mechanism (they fill when water overflows from the deeper channels on the outer edges of the dams). The 1 m spatial resolution of the DEM provides high spatial detail while remaining computationally efficient for the modelling of each dam.

2.3 Satellite systems

Satellite remote sensing has the unique benefit of providing regular, high-coverage observations during the lifetime of a satellite mission. A variety of satellite systems enable the monitoring of wetland hydrological parameters (Guo et al., 2017; Sudriani et al., 2023). These include passive systems (e.g. optical sensors) that detect the sunlight reflecting from the Earth's surface, and active systems (e.g. SAR sensors) that send pulses of energy to the Earth's surface and detect their return. Passive systems such as Sentinel-2 can monitor water extent and water quality, while active sensors such as SWOT can detect water extent and additionally water surface elevation.

2.3.1 Sentinel-2

The Sentinel-2 satellites provide optical imagery globally at a resolution of 10-20 m, every 3-10 days since 2015 (Drusch et al., 2012). The satellites carry multi-spectral sensors that detect the sunlight that reflects from the Earth's surface in 13 spectral bands across the visible, near-infrared and shortwave-infrared wavelengths. Sentinel-2 has been widely used to quantify surface water extents globally due to its high spatial resolution and frequent revisit time (e.g. Miura et al. (2025)).

Sentinel-2 water detection

Index-based approaches are most commonly used for water detection using multi-spectral satellite data such as Sentinel-2 data as they are simple and cost-effective (Nagaraj & Kumar, 2024; Zhao et al., 2025). These involve the calculation of spectral indices, which

are combinations of surface reflectance across different spectral bands, that are designed to optimise the detection of particular features on the land surface. For water detection, a threshold can be applied to the spectral index in order to retain only pixels with a high likelihood of being water. The optimal index and threshold to classify water-covered areas can vary significantly within and across wetlands, as the spectral properties of wetland land and water surfaces often change over space and time (Gallant, 2015). Nevertheless, spectral index-based water detection approaches are widely used in wetland monitoring globally.

The Normalised Difference Water Index (NDWI) is one of the earliest multi-band water detection indices (McFeeters, 1996). It leverages the infrared-absorbing property of water by combining the surface reflectance in the green and near-infrared bands to enable the discrimination of water surfaces. A modification to the NDWI was proposed by Xu (2006), who developed the Modified Normalised Difference Water Index (MNDWI) that uses shortwave-infrared reflectance instead of near-infrared, to enhance the delineation of water in mixed land cover. The MNDWI has been widely used for detecting water in inland water bodies globally, using a threshold of 0 or -0.3 (Sims et al., 2014; Du et al., 2016; Slagter et al., 2020). The Tasseled Cap Wetness (TCW) index is another spectral index designed to detect water (Crist, 1985), and has been used with thresholds of -0.035 and 0. It has yielded improved detection of water under vegetation, prompting its use for mapping wetland inundation (Dunn et al., 2019; Ticehurst et al., 2022; Ouma & Tateishi, 2006). Ticehurst et al. (2022) found that the TCW was superior to other indices for detecting water in floodplain wetlands in the Murray-Darling Basin. Figure 2.3 shows the water extents obtained using the MNDWI (Figure 2.3a and 2.3b) and TCW index (Figure 2.3c and 2.3d) with commonly used threshold values. This figure highlights the importance of determining an optimal threshold value for detecting water-covered areas.

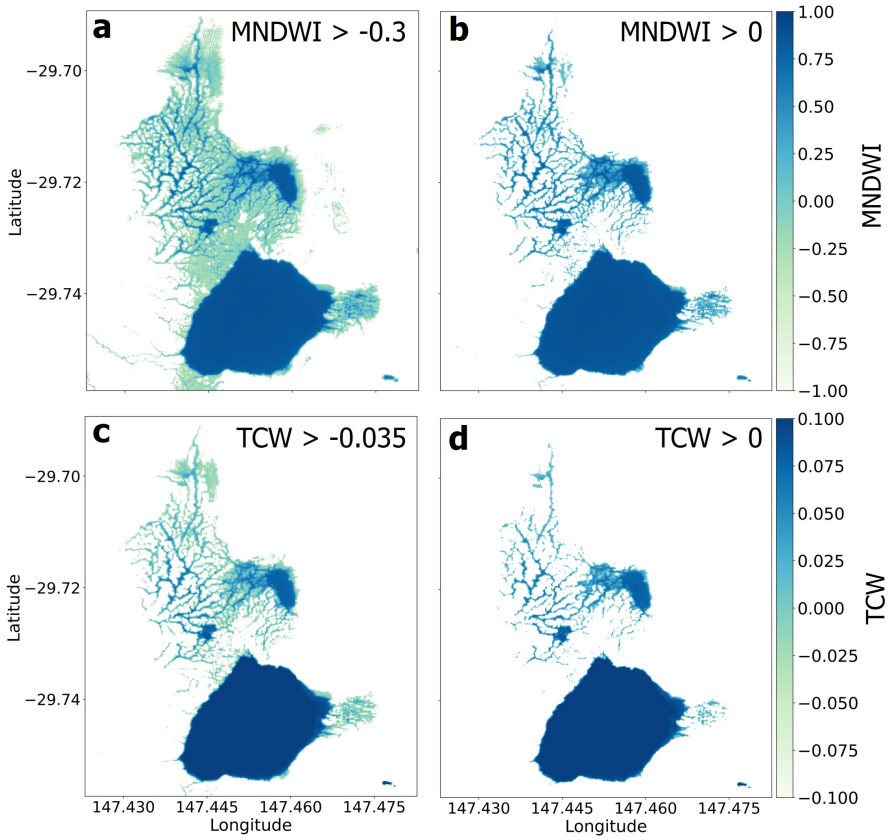


Figure 2.3: Water extent (non-white pixels) across the Narran Lakes wetland using the MNDWI with thresholds of **(a)** -0.3 and **(b)** 0, and the TCW index with thresholds of **(c)** -0.035 and **(d)** 0.

Limitations of Sentinel-2 water detection

The water detection capability of Sentinel-2 and other optical satellite sensors is impacted by several factors. Importantly, optical sensors cannot observe the Earth's surface in cloudy conditions (e.g. Figure 2.4) and during the night. This substantially reduces the number of usable satellite images over a study site, particularly in tropical regions where it is often cloudy, and during flood events coinciding with local rainfall and cloudy conditions (Ozesmi & Bauer, 2002).

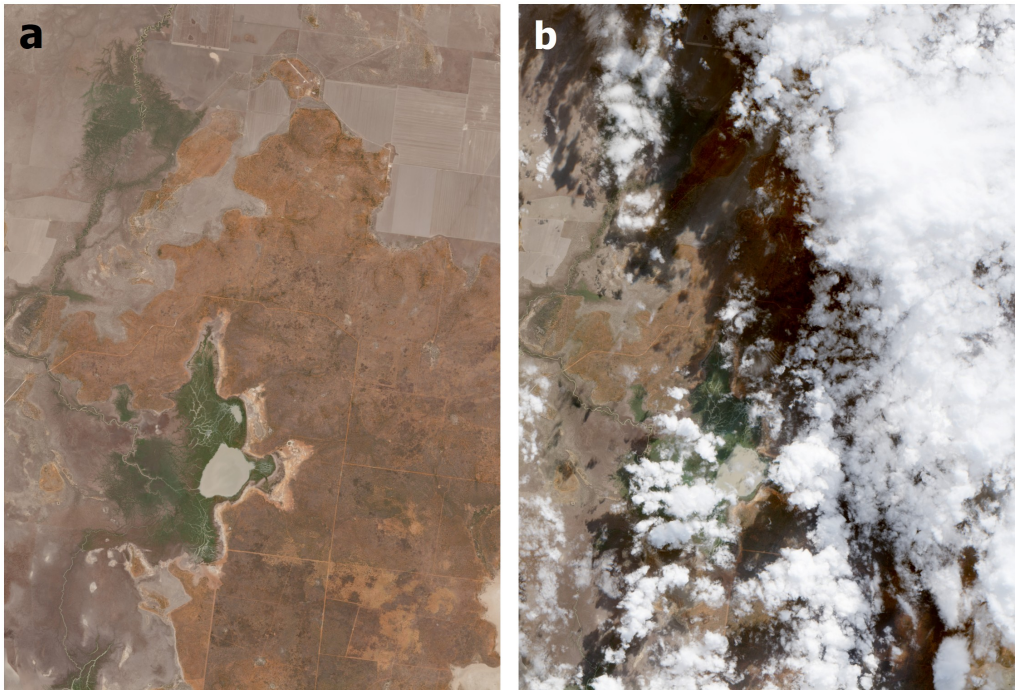


Figure 2.4: Example of a **(a)** clear and **(b)** cloud-covered Sentinel-2 image over the Narran Lakes wetland region, on 9 May 2026 and 26 May 2026 respectively.

As discussed in Section 2.1, the spatial heterogeneity of wetland landscapes creates a challenge for water detection tools (Gallant, 2015; Ma et al., 2019). Optical water detection indices rely on distinguishing distinct spectral signatures (i.e. reflectance of a surface in different wavelengths) from different land surfaces. However, 'mixed' pixels in wetlands that contain a mixture of bare soil, vegetation and water (e.g. at a land-water boundary or water with submerged or emergent vegetation) contain mixed spectral signatures, making them difficult to accurately distinguish as water or non-water (Heath et al., 2024). Furthermore, vegetation may partially or fully obscure a water surface, leading to potential misclassification of the area if its spectral signature is dominated by the vegetation. As mentioned, specialised spectral indices such as the TCW index may mitigate this issue (Ticehurst et al., 2022), but their effectiveness remains highly site-specific (Fisher et al., 2016). Furthermore, many authors have developed more complex water detection algorithms that incorporate multiple spectral bands and indices (e.g. Ticehurst et al. (2022); Lefebvre et al. (2019)), or automated adaptive thresholding (e.g. Che et al. (2025); Günen and Atasever (2024)), but these methods may also yield varied results across different study sites.

Despite the limitations of Sentinel-2 water detection, its high spatial and temporal resolution and global coverage makes it a useful water detection tool. I chose to use Sentinel-2 data in my study for these reasons, and additionally because there were no in situ or airborne water detection tools available for my study. The 20 m spatial resolution of the Sentinel-2 images is comparable to the SWOT PIXC pixels (which are different sizes but approximately 22 m by 10-60 m), providing a suitable reference against which to

compare SWOT-derived water extents. As shown in the Narran Lakes wetland in Figure 2.3, the water extents obtained using the MNDWI and TCW index at different threshold values can vary substantially. The choice of threshold can be made through comparisons with independent water extent datasets such as other satellite data, airborne imagery, modelled water extents, or in situ mapping. In my study, I developed a novel method to compare the water extents across the farm dams using the MNDWI and TCW index at different thresholds against modelled water extents derived from a GIS-based fill model (see Section 3.3).

2.3.2 SWOT

The Surface Water and Ocean Topography (SWOT) satellite mission, launched in December 2022, offers unprecedented capabilities for hydrological monitoring compared to existing satellite sensors (Biancamaria et al., 2016). It operates using interferometric SAR, by sending pulses of Ka-band radar energy to the Earth's surface simultaneously from two antennas and calculating the time for the energy to scatter back to both sensors. Since both antennas simultaneously observe two regions (or 'swaths') of the Earth, the system can calculate the absolute height of each point in the swath using the difference in return time between the backscatter (i.e. energy scattered back from the Earth) captured from each antenna. SWOT's Ka-band Radar Interferometer (KaRIn) has a wavelength of 8.6 mm and operates at near-nadir incidence angles (i.e. the viewing angle is almost perpendicular to the Earth's surface, between ∼0-4 °), producing strong backscatter over water bodies. Using this technique, water surface elevations over inland water bodies can be measured with centimetre-scale accuracy, at a high spatial resolution and at least every 21 days (Maubant et al., 2025; Kica et al., 2025; Girard et al., 2025; Salameh et al., 2026).

The SWOT mission provides several pre-processed data products that can be used for continental hydrological analyses. The foundational 'Level 2' product (processed from the raw radar measurements) is the Pixel Cloud (PIXC) product, which provides height estimates of land and water surfaces on pixels that are ∼22 m along-track (parallel to the satellite flight direction) by 10-60 m cross-track (perpendicular to the satellite flight direction) (Surface Water Ocean Topography (SWOT), 2025). A Raster product is also available, which aggregates the PIXC data on a regular 100 m or 250 m grid. Finally, two high-level spatial products are available, which are vector datasets of aggregated PIXC height estimates and other variables over pre-defined lake polygons or river reaches and nodes. Given that the PIXC product provides the foundational data for the Raster and spatial products, any errors in the PIXC product will be propagated to the higher level products. Furthermore, the PIXC product is the most frequently used and well-suited SWOT data product for monitoring wetlands and smaller water bodies (Maubant et al., 2025; Kica et al., 2025; Callaway et al., 2026; Shirafkan et al., 2026; Beltrão et al., 2026). Therefore, it is most important to assess how well water surfaces are detected in the PIXC product.

SWOT water detection

Along with a height estimate, each PIXC pixel also contains additional information about its radar parameters, the land cover it represents, the quality of the data, and its area. One of the key radar parameters provided is the coherent power received from each pixel. This parameter is the combination of the coherent (i.e. stable) backscatter received from both antennas, which is then used to derive the pixel's height estimate. Coherent power is sensitive to surface characteristics (Bonassies et al., 2026). Due to the near-nadir viewing geometry of the SWOT satellite, the coherent power received is highest over smooth water surfaces that produce specular reflectance of the majority of the signal back to the sensor. Rougher surfaces generally cause increased scattering of the signal away from the sensor which decreases the coherent power. Sufficiently high coherent power is required for the radar signal to be correctly processed in the SWOT algorithm and, subsequently, to yield an accurate height estimate over an area.

The PIXC data also includes a built-in classification algorithm that assigns each pixel to a land cover class based on its coherent power and whether it has been classified as water in independent datasets of global water bodies (JPL D-105504, 2023). These classes include 'land', 'land near water', 'water near land', 'open water', 'dark water', 'low-coherence water near land' and 'open low-coherence water'. Simply put, pixels in each SWOT image with sufficiently high coherent power and high likelihood of being water according to the independent information will be classified as 'open water' (with the caveat that this classification process involves additional complex spatial regularisation). Pixels are generally assigned to 'low-coherence' classes if they are affected by issues such as layover (geometric distortion due to steep land elevation), vegetation, or other surface scattering effects, which lead to inaccurate water surface elevation measurements in most cases (Karami et al., 2026; JPL D-105504, 2023). Analysis of PIXC data typically involves the selection of 'open water' and/or 'water near land' pixels to retain only pixels that yield accurate water surface elevation estimates (Maubant et al., 2025; Callaway et al., 2026; Masoumi & Tourian, 2026; Karami et al., 2026).

Additionally, each pixel contains data quality flags, which are bit-mapped values describing any quality issues affecting each pixel (e.g. issues with geolocation, classification, or measured radar parameters). In order to obtain accurate and reliable water surface elevation estimates from the PIXC data, the pixels should be filtered to retain only high quality pixels. Several studies have proposed suitable filtering methods for this purpose (e.g. Maubant et al. (2025); Callaway et al. (2026)).

Limitations of SWOT water detection

Given that SWOT is the first spaceborne KaRIn sensor in operation, there were initially uncertainties about its ability to detect water in wetland conditions (Desrochers et al., 2021). Preliminary studies assessing simulations of SWOT-like backscatter using AirSWOT measurements (an airborne Ka-band experimental instrument developed prior to

the launch of SWOT) showed that both surface moisture and vegetation are likely to impact SWOT water detection (Fayne et al., 2024; Desrochers et al., 2021). Specifically, Fayne et al. (2024) found that while open water is generally distinguishable from dry land, it may be challenging to distinguish between water and vegetated littoral zones (i.e. shoreline areas) or wet soil, as these surfaces have high moisture that can in some cases yield backscatter values comparable to water surfaces. Desrochers et al. (2021) found that, while underwater aquatic vegetation had a negligible impact on SWOT backscatter, the backscatter from areas with emergent vegetation (i.e. vegetation growing above a water surface) was, in some cases, similar to surrounding wet soil areas. This was both because the surrounding soil was very wet and also because vegetation can cause volumetric scattering of the incoming signal, decreasing the backscatter received by the sensor. Importantly, both of these studies highlight that the impacts of vegetation and surface moisture on SWOT water detection are likely to vary spatially between different land cover types and temporally across wet and dry seasons, necessitating caution when interpreting SWOT results in wetlands.

Since the launch of the SWOT mission, various studies have assessed the accuracy of SWOT water extent estimates from several of the available data products. Most authors agree that the performance of SWOT in environments affected by vegetation, mixed pixels and rapidly changing hydrological conditions can be complex and site-specific (Beltrão et al., 2026). Bonassies et al. (2026) found that while the SWOT PIXC built-in classification accurately detected flood extents in forested areas in some cases, in other cases its accuracy was significantly limited by environmental and observational parameters (e.g. wind and incidence angle). Furthermore, they found that SWOT was overly sensitive to soil moisture during flood recession periods (Bonassies et al., 2026). In Australian wetlands, assessments of SWOT water extents are currently limited. Callaway et al. (2026) found that the SWOT PIXC data delineated water in both a river red gum forest and a shallow, semi-arid wetland system, but found cases where land on the edges of the water bodies was misclassified as water.

Other assessments of SWOT water extents use the Raster product, as it provides data with a spatial resolution and alignment that is more easily comparable to existing satellite-based raster datasets (e.g. Sentinel-2). While the Raster product lacks the spatial detail of the PIXC data, it can nevertheless reveal cases where the underlying SWOT water detection algorithm may fail. For instance, several assessments of the SWOT Raster product in vegetated floodplains found that it detected larger water extents compared to optical satellite-based observations (Salameh et al., 2026; Bhattarai et al., 2026). In some cases, this was attributed to misclassifications of vegetated water areas as non-water in the optical datasets (Salameh et al., 2026), while in others this was attributed to misclassifications of non-water areas as water by SWOT (Bhattarai et al., 2026). Given these mixed results, it is clear that the ability of SWOT to detect water in wetlands is complicated, and that validating SWOT using other datasets can be challenging due to the inherent difficulties in detecting water in wetlands with any remote sensing tool. In view of this challenge,

my study of several large, vegetated farm dams in Australia provides a more controlled environment in which to assess SWOT's performance. The dams contain similar ecological and hydrological features as natural Australian wetlands, including temporary inundation of herbaceous and woody vegetation, but with less hydrological and topographic complexity, making these useful test sites for comparing SWOT PIXC water extents with other satellite-based and modelled water extents.

Along with land surface characteristics, the incidence angle of SAR observations also impacts the backscatter received from a surface (Lang et al., 2008; O'Grady et al., 2013). While SWOT operates at a small range of near-nadir incidence angles (∼1-4°), differences in incidence angle within this range can introduce substantial variation in the backscatter received from individual PIXC pixels. This can occur because pixels located towards the inner part of each swath are observed at smaller incidence angles than pixels on the outer parts of the swath (Figure 2.5). Furthermore, the flight path of the SWOT satellite produces some regions where several swaths partially overlap, but at different orientations. This yields observations of the same area at different incidence angles.

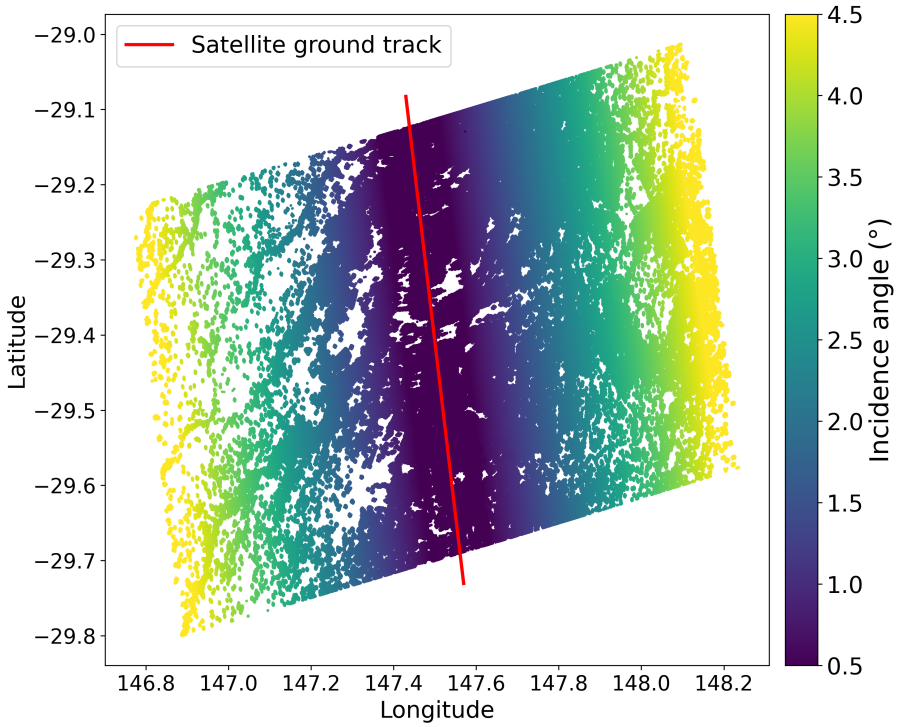


Figure 2.5: Incidence angles of each pixel in two SWOT PIXC tiles on the left and right sides of the satellite ground track (i.e. the path on the Earth's surface below the satellite's flight path).

Within the range of SWOT incidence angles, studies have found that the backscatter from water surfaces decreases with increasing incidence angle (due to increased reflectance of the signal away from the sensor at larger incidence angles) (McQuillan et al., 2025; Desrochers et al., 2021; Bonassies et al., 2026). However, this relationship is influenced by environmental conditions such as wind (Fayne et al., 2024; Desrochers et al., 2021;

Bonassies et al., 2026). Wind produces roughness on water surfaces, which causes the signal to scatter in all directions as it bounces off the water. At small incidence angles, backscatter decreases with increasing wind speed, as less signal is specularly reflected directly back to the sensor. At larger incidence angles, backscatter increases with increasing wind speed, as some of the signal is scattered back to the sensor (as opposed to the complete specular reflectance of the signal away from the sensor that typically occurs at large incidence angles over still water) (McQuillan et al., 2025). These effects impact the pixel classification algorithm and may cause the misclassification of water surfaces as non-water if the backscatter (and associated coherent power) received by the sensor is too low due to the combination of incidence angle and wind conditions in a particular epoch. In my study, the observations of the farm dams from all available SWOT passes had incidence angles of $\sim 3^{\circ}$, but there were no available in situ wind speed data to assess potential wind-induced effects. Nevertheless, these effects can constrain radar-based water detection over open water bodies generally.

Chapter 3

Constraints on the accuracy of SWOT water detection in wetlands

I initially assessed the ability of SWOT to detect water in the Narran Lakes wetland, a semi-arid terminal wetland system in northern NSW. By comparing the SWOT water extents with Sentinel-2 optical imagery and in situ river gauge data, I found inconsistencies in the accuracy of the SWOT water detection. Specifically, there were several cases where SWOT incorrectly classified water areas as non-water. To investigate these issues, I undertook a controlled test study in the vegetated farm dams of Cubbie Station. This chapter is based on the manuscript under review in Geophysical Research Letters:

Taib, M. and Tregoning, P., 2026. Constraints on the accuracy of SWOT water detection in wetlands, manuscript submitted to *Geophysical Research Letters* on 7 September 2026.

I made the following contributions to this paper:

- Analysed Sentinel-2 MNDWI and SWOT PIXC data over Narran Lakes wetland (Section 3.1).
- Developed a method to separate standing water pixels and likely wet soil pixels from all SWOT PIXC high quality water-classified pixels (Section 3.2.3 and 3.4)
- Developed a fill model to simulate water extents across the farm dams (Section 3.2.5)
- Assessed the similarity between Sentinel-2 MNDWI and TCW index water extents across the partially filled dams at different thresholds, against the fill model water extents on the corresponding days (Section 3.3)
- Developed a raster-based method to assess the accuracy of the SWOT water detection under different canopy heights, by comparing spatially aligned SWOT PIXC data to a vegetation height model (Section 3.5)
- Compared SWOT water extents with fill model water extents, coherent power and canopy height across a subset of the dams (Section 3.5)
- Wrote the text and created all the figures for the manuscript

Key points

- Misclassifications of water and non-water areas occur in SWOT PIXC data.
- SWOT detects wet soil as water.
- Emergent vegetation sometimes correlates with missed SWOT water detections.

Abstract

Monitoring the extent and depth of water within wetlands is important for managing these vulnerable ecosystems. The Surface Water and Ocean Topography (SWOT) satellite mission measures water levels across wetlands every ∼11-21 days. However, the ability of SWOT to even detect water accurately is complicated by surface conditions such as soil moisture and emergent vegetation, affecting the utility of SWOT data in wetland environments. Here we assessed SWOT pixel cloud water extents in large farm dams in Australia against water extents from a fill model and Sentinel-2 water indices. We found cases where SWOT misclassified wet soil as open water, and cases where SWOT misclassified water as land when the vegetation canopy height extended above the water surface. While the interactions between surface parameters and SWOT water detection are complex, SWOT nevertheless provides valuable, new insights into changing water availability across wetland environments.

Plain Language Summary

Wetlands depend on water to function. Monitoring the water within wetlands is therefore critical for managing the vulnerable ecosystems wetlands support. The new Surface Water and Ocean Topography (SWOT) satellite mission can accurately measure water heights in wetlands. However, research has found that its ability to detect water on the Earth's surface becomes complicated in areas of wet soil and flooded vegetation, which are common in wetlands. Our study compares SWOT data to a model and other satellite data to assess how well SWOT can identify water in large farm dams in Australia. We found cases where SWOT mistook wet soil for water, and cases where SWOT did not detect water underneath tall vegetation canopies. The interactions between the conditions on the land surface and the ability of SWOT to detect water are complex, but SWOT can nevertheless provide useful observations of water in wetlands.

3.1 Introduction

Increasing anthropogenic impacts on the global water cycle are threatening freshwater environments such as wetlands (Falkenmark et al., 2019; Reid et al., 2019; Capon et al.,

2021). Monitoring the extent, depth and frequency of inundation within these environments is critical for maintaining and managing the ecological, social and economic value they provide (Robertson et al., 2025; Gallant, 2015).

Remote sensing tools offer insights into hydrological changes in wetlands. For example, the Sentinel-2 optical satellite sensors provide frequent, high spatial resolution imagery that can detect water extents accurately (Heath et al., 2024; Lefebvre et al., 2019; Kordelas et al., 2019). Wetland inundation extent has also been monitored by combining optical imaging with radar techniques capable of all-weather monitoring (Bourgeau-Chavez et al., 2009; Gašparović & Klobučar, 2021). Prior to the launch of the Surface Water and Ocean Topography (SWOT) satellite mission, estimates of water levels in wetlands could only be made indirectly using water extent measurements combined with land elevations from Digital Elevation Models (DEM) (Usman et al., 2025; Penton et al., 2023).

The SWOT satellite, launched in 2022, provides direct measurements of water surface elevations in wetlands with high spatial resolution (10-60 m by ∼22 m) every 11-21 days (Kica et al., 2025; Callaway et al., 2026). However, preliminary studies of simulations using AirSWOT (SWOT's airborne experimental precursor) predicted that distinguishing land from water in littoral zones with high soil moisture and emergent vegetation using SWOT may be challenging (Desrochers et al., 2021; Fayne et al., 2024). Since the launch of SWOT, Kica et al. (2025) found that SWOT accurately measured water surface elevation in herbaceous wetlands, but recommended further evaluation in wetland types with denser vegetation. Callaway et al. (2026) similarly found that SWOT can delineate the boundaries of semi-permanent wetlands, but that water surface elevation anomalies increase at lake edges. Finally, Bonassies et al. (2026) found that while SWOT detected flooding in forested areas, it struggled to distinguish between open water areas and high soil moisture.

We found that SWOT's ability to detect water in an Australian wetland system varied substantially in the Narran Lakes wetland in Northern NSW, Australia. While the inundation of this wetland was observed well by SWOT in some cases (e.g. the flood event in Figures 3.1a-c), sometimes SWOT did not detect water across most of the wetland (Figures 3.1d-f), including when Clear Lake was full of water according to Sentinel-2 satellite observations (Figures 3.1d and 3.1e). This missed detection likely occurred due to the low water levels in the lake that were obscured by emergent vegetation (which can be seen in the green areas in Clear Lake in Figure 3.1d). The ability of SWOT to detect water in vegetated environments is therefore complicated, and this must be better understood in order if one is to utilise SWOT observations with confidence in diverse wetlands globally.

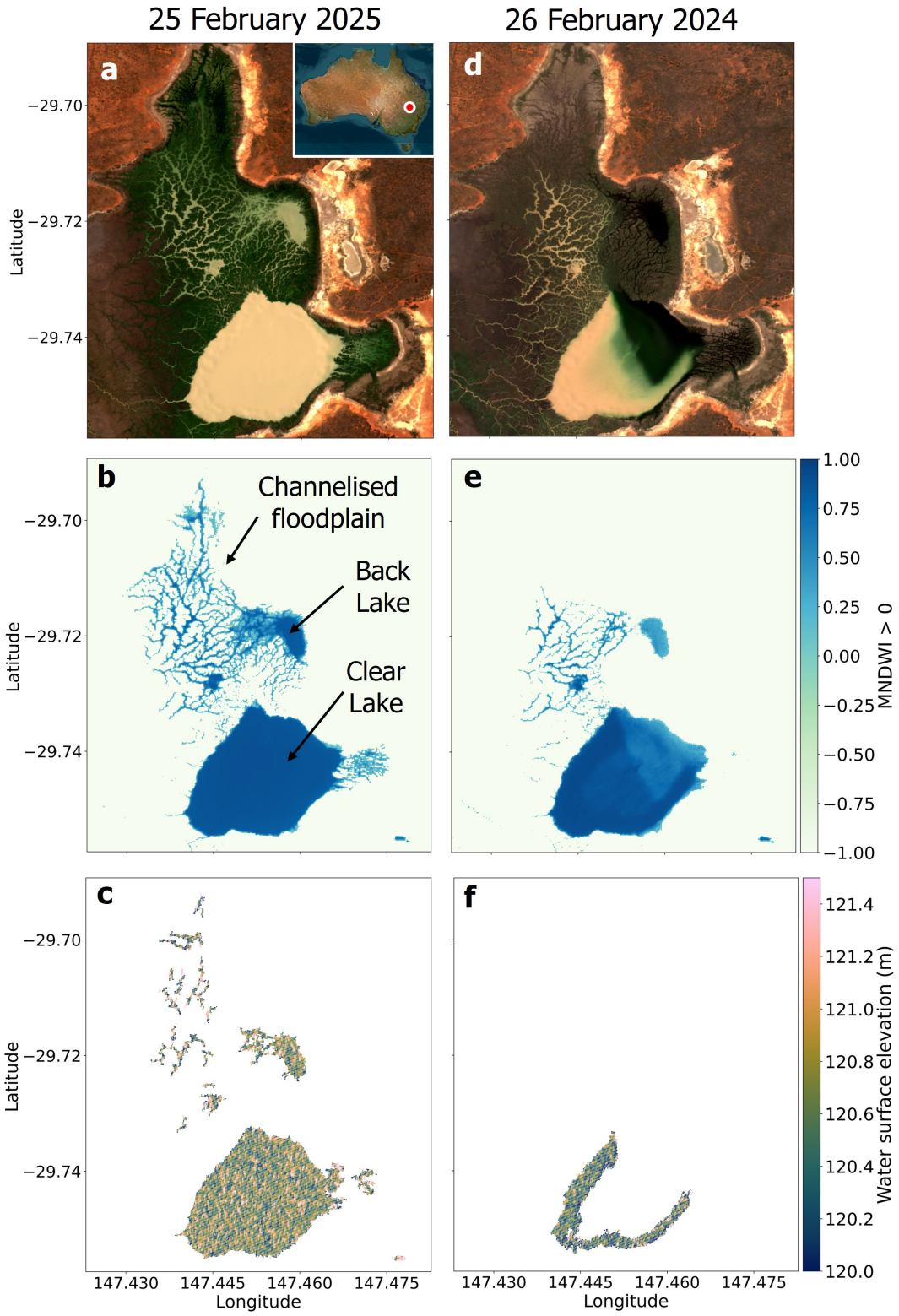


Figure 3.1: Narran Lakes wetland **(a-c)** during a flood event on 25 February 2025 and **(d-f)** at the beginning of a different flood event on 26 February 2024: **(a,d)** Sentinel-2 optical image, **(b,e)** MNDWI thresholded at 0, and **(c,f)** SWOT pixel cloud water surface elevations of good quality water pixels. The SWOT data identify the full Clear Lake in 2025 **(c)** but not in 2024 **(f)**.

In this study, we test the capability of the SWOT satellite to identify water-covered land surfaces in large farm dams in southern Queensland, Australia (∼100 km north-east along-track from Narran Lakes), where water depths change significantly and often. We assess the impact of emergent vegetation on the SWOT water detection and identify cases where SWOT classifies wet soil as water.

3.2 Data

3.2.1 Study site

We assessed SWOT water detection across a set of seven large (∼4.5-16 km^2), vegetated farm dams on Cubbie Station, located in the Condamine-Balonne catchment in the northern Murray-Darling Basin (Figure 4.1). According to SWOT water surface elevation measurements, the water levels in these dams varied by up to 6 m throughout 2024-2026, providing an opportunity to assess SWOT's water detection capability at a range of depths, including when the dams were only partially full. The dams have mixed land covers, including almost bare soil, grass cover, low shrubs, and sparse trees. The gently sloping topography within each dam means that small changes in water level create large changes in spatial water extent, facilitating comparisons between water extents detected by SWOT and other methods.

3.2.2 Dam bathymetry

We obtained a 1 m Digital Elevation Model (DEM) of the farm dams derived from an airborne Light Detection and Ranging (LiDAR) survey of the lower Balonne River conducted in December 2018 (State of Queensland Department of Natural Resources, Mines and Energy, 2019). The survey was conducted during a drought period when all dams were empty. LiDAR land heights are provided in the Australian Height Datum 1971 (AHD) relative to the AUSGeoid09 and have a quoted vertical accuracy of ±0.3 m.

3.2.3 SWOT water detection

We used the Version D SWOT Pixel Cloud (PIXC) product from January 2024 to January 2026. This product provides geolocated height estimates on pixels that are ∼22 m in the along-track direction and 10-60 m in the cross-track direction, with a 21-day revisit time. These heights are provided relative to the WGS84 reference ellipsoid and were corrected for tidal effects (which are provided with the PIXC data (JPL D-109532, 2025)), and converted to AHD heights. The only available SWOT passes over the study site yielded pixels with incidence angles of ∼3° over the dams.

Each PIXC pixel includes information on the KaRIn backscatter and coherent power received from the pixel (JPL D-105504, 2023), along with a built-in classification based on the coherent power and additional independent information about prior known locations of water features. The built-in classification provides a simple method for users to retain only

water pixels for subsequent analyses, such as by selecting only pixels classified as 'open water' and/or 'water near land'. We retained these pixels but also applied the filtering approach of Callaway et al. (2026) to consider the accompanying pixel quality flags when identifying good quality water pixels.

The identified good quality pixel heights are then aggregated to obtain high accuracy estimates of mean water surface elevation across a water body, weighted by the individual pixel areas (Maubant et al., 2025; Callaway et al., 2026). To mitigate the risk of including contaminated shoreline pixels in the estimates of water surface elevation, we used only pixels with coherent power greater than the highest peak of the coherent power distribution of the good quality water pixels (subsequently referred to as the 'High Coherent Power (HCP)' water pixels). While this approach excludes some valid standing water pixels with slightly lower coherent power, it identifies a subset of the pixels that we are confident are standing water. This process is described further in Section 3.3.

3.2.4 Simulated water extent

We developed a simple water fill model using the DEM and the mean SWOT water surface elevations to model the spatial extent of the filling of the dams. For each epoch and each dam, we first created a binary mask of the DEM to select all pixels with land elevations lower than the mean SWOT water surface elevation of the 'HCP' water pixels. For each dam, we selected a low-elevation seed point and then retained only the group of selected DEM pixels connected to the seed point, to mimic the filling of the dam from this point. This created simulations of the area of each dam that would be covered with water at each epoch for a given mean water surface elevation estimate from available SWOT data. We subsequently used this spatial extent to assess the accuracy of the Sentinel-2 and SWOT water detections.

3.2.5 Sentinel-2 water extent

The Sentinel-2 sensors are commonly used for water detection in wetland environments and offer 10-20 m spatial resolution. Water detection is typically achieved using spectral indices such as the Modified Normalised Difference Water Index (MNDWI) (Xu, 2006), which combines the green and shortwave-infrared reflectance bands. The Tasseled Cap Wetness index (TCW) (Crist, 1985) has also been used in Australian wetlands (Dunn et al., 2019; Ticehurst et al., 2022). We obtained analysis-ready Sentinel-2 images every 2-3 days from the Digital Earth Australia platform (Geoscience Australia, 2022a, 2022b, 2022c), from which we calculated the MNDWI for cloud-free epochs from January 2024 to January 2026 (details of this process are provided in Section 4.1).

MNDWI threshold values, above which pixels are considered to be water, vary and have included -0.3 (Sims et al., 2014) through to 0 (Xu, 2006; Miura et al., 2025). Water extents obtained from the MNDWI are validated through comparisons with independent water extent datasets (Xu, 2006) or with other remote sensing data such as airborne or satellite imagery (Feyisa et al., 2014; Sims et al., 2014; Ticehurst et al., 2022). This can be

time consuming and often relies solely on optical detection systems, which are ineffective in cloudy conditions.

We compared the water extents obtained from the MNDWI at different thresholds to the water extents obtained from the fill model described in Section 3.2.4 on days when both SWOT and Sentinel-2 showed partially full dams. This validated both the MNDWI threshold values and the fill model water extents, which could then be used to assess the SWOT water detection. A similar process using the fill model and the TCW index yielded comparable results (see Section 4.2, Section 4.3 and Figure 4.3).

3.2.6 Vegetation cover

Desrochers et al. (2021) suggested that emergent riparian vegetation impacts KaRIn water detection, which is a possible explanation for the missed SWOT water detections in Figure 3.1f. To test this, we assessed the ability of SWOT to detect water in the dams when vegetation protruded through the water surface. We obtained an Australia-wide annual dataset of vegetation height estimates for 2024 (Ticehurst et al., 2025; Ticehurst & Newnham, 2024), which provides top-of-canopy height estimates on 30 m pixels across the dams. We resampled this dataset to 1 m pixel resolution and added the vegetation heights to the DEM heights to obtain an AHD canopy height raster.

3.3 Comparison of fill model water extents with Sentinel-2 water extents

We first compared the water extents generated using different MNDWI thresholds to the water extents generated using the fill model in several partially full dams. We quantified the similarity between these rasters using the Jaccard index (Jaccard, 1901) (see Section 4.3 for details of this method).

Although the MNDWI thresholds that yielded the optimal similarity to the fill model water extents varied between dams and epochs (Figure 4.2a), our results confirmed the range used in the literature for water detection in wetlands, which is generally between -0.3 and 0 (Xu, 2006; Miura et al., 2025; Sims et al., 2014; Ticehurst et al., 2022). There was good consistency between the fill model and the MNDWI for most dams (Jaccard index $> \sim 0.9$), except in cases where receding water produced puddles with high MNDWI that were not simulated by the fill model (light blue, grey, pink and orange epochs in Figure 4.2a). Excluding these cases, the MNDWI validated the fill model water extents, justifying the use of the fill model for subsequent assessments of SWOT water extent, even in cloudy conditions where Sentinel-2 observations were unavailable.

3.4 SWOT detection of shallow water and wet soil

On 04 January 2024, the SWOT pixels across most of Cubbie 7 (non-white pixels in Figure 3.2a) were classified as 'open water' or 'water near land'. It is clear, however, that the water surface elevations of these pixels do not form a flat, standing water surface, as they have an increasing gradient across the dam consistent with that of the land elevation (Figures 3.2b and 3.2c). This suggests that pixels classified as water across the dam are not standing water, but rather are most likely wet soil or puddles of very shallow water. The MNDWI across the dam two days prior to the SWOT pass was low (mean = -0.37 $\pm$ 0.02), and continued to decrease during the following week (down to a mean = -0.41 $\pm$ 0.03), indicating that the dam was drying out. This strongly suggests that the SWOT water pixels were, in fact, wet soil pixels on 04 January 2024. It is clear that care should be taken when interpreting the water surface elevation estimates on apparently good quality, water-classified SWOT pixels, as they may not always represent a standing water surface.

We now look in detail at a case of a partially-filled Cubbie 1 dam (Figures 3.2d-i). The bathymetry of the dam has a $\sim$1.5 m slope along the transect in Figure 3.2i (marked with an arrow in Figure 3.2d). The water area on the western side of the dam (light blue and dark blue pixels in Figures 3.2d, 3.2i) is deeper and forms a standing water surface (albeit $<$ 1 m deep). Among these pixels, we can identify a group of 'HCP' pixels with coherent power greater than 80.44 dB (light blue pixels in Figure 3.2g), which we are confident represent the standing water surface. Compared to these pixels, the water pixels in the centre of the dam (yellow pixels in Figure 3.2d) have substantially lower coherent power (Figures 3.2e, 3.2g, 3.2i), and they lie on land with elevation above the mean water surface elevation of the standing water 'HCP' pixels. This suggests that the group of pixels in the centre of the dam are not standing water but are likely wet soil. However, both groups of pixels were classified as 'open water' or 'water near land', even though the wet soil pixels have a higher mean with a larger spread (159.52$\pm$0.36 m) than the 'HCP' water pixels (159.43$\pm$0.12 m) (Figure 3.2h). The fill model using the mean water surface elevation of the 'HCP' water pixels, uncontaminated by likely soil moisture pixels, therefore shows the extent of the standing water surface and excludes the wet soil pixels (Figure 3.2f).

3.5 Impact of vegetation on SWOT water detection

To assess the accuracy of the SWOT water detection through emergent vegetation, we conducted a pixel-by-pixel raster analysis between the SWOT water extent and the canopy height above the water surface. We first subtracted the mean SWOT water surface elevation estimate from the AHD canopy height raster to obtain a raster of the height of emergent vegetation. We then separated this raster into several 'binned' rasters containing the pixels with specific canopy heights above the water (shown in Figures 3.3b-i).

We rasterised the SWOT pixels onto the 1 m grid of the canopy height rasters (details of this method are provided in Section 4.5). We then assessed the accuracy of the SWOT water detection for each canopy height above the water bin by calculating the proportion

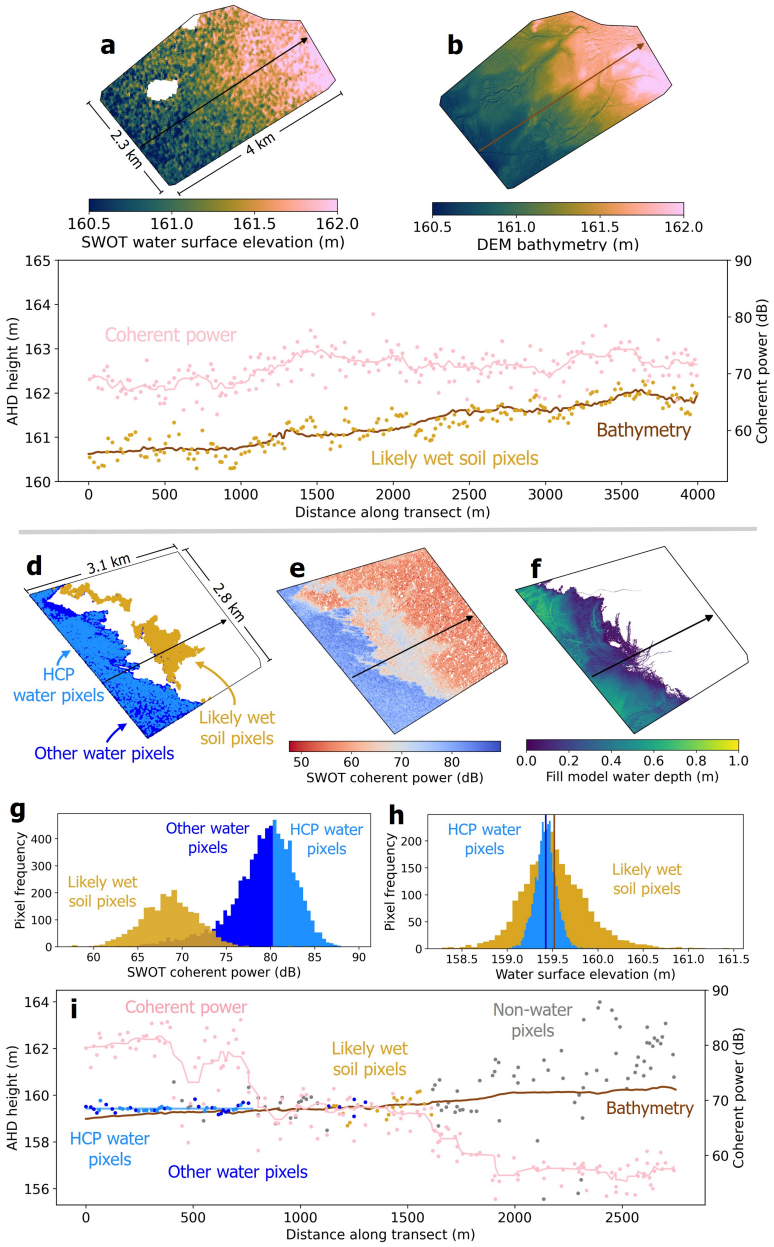


Figure 3.2: **(a-c)** Cubbie 7 dam on 04 January 2024: **(a)** Water surface elevation of all water-classified SWOT pixels and **(b)** DEM bathymetry. **(c)** Transect of DEM bathymetry and water surface elevations and coherent power of water-classified SWOT pixels (see Section 4.4 for a description of how the transects were calculated). **(d-i)** Cubbie 1 dam on 17 March 2025: **(d)** Spatial extent of all water-classified SWOT pixels, including SWOT 'High Coherent Power (HCP)' pixels (light blue), likely wet soil pixels (yellow) and other water pixels (dark blue), **(e)** SWOT coherent power of all pixels, and **(f)** simulated water depth using the mean water surface elevation of the 'HCP' water pixels. **(g)** Coherent power of 'HCP' water pixels, likely wet soil pixels and other water pixels. **(h)** Water surface elevation of 'HCP' water pixels and likely wet soil pixels. The means of the 'HCP' pixels (159.43±0.12 m) and wet soil pixels (159.52±0.36 m) are shown with a blue and brown vertical line, respectively. **(i)** Transect of DEM bathymetry, and coherent power and water surface elevations of SWOT water pixels (including 'HCP' pixels and their mean water surface elevation, likely wet soil pixels and other water pixels) and non-water pixels.

of the pixels in each canopy height bin (hatched pixels in Figures 3.3b-h) that SWOT detected as water (from the blue pixels in Figure 3.3a). Before calculating this accuracy, we masked the binned canopy height rasters to retain only the area within the 'true', fill model water extent to ensure that no SWOT false positives (i.e. non-water pixels that SWOT incorrectly identified as water) influenced the assessment.

The SWOT water detection accuracy generally decreased with increasing vegetation height above the water (Figure 3.3i). This was observed in the Cubbie 1 and Cubbie 2 examples, although the canopy height at which the degradation began varied for different epochs. However, the interaction between canopy height above the water and SWOT water detection accuracy is clearly complex, since the Cubbie 3 example showed that SWOT could sometimes detect water in the areas with the highest canopy above the water (e.g. 08 May 2024 in green in Figure 3.3i).

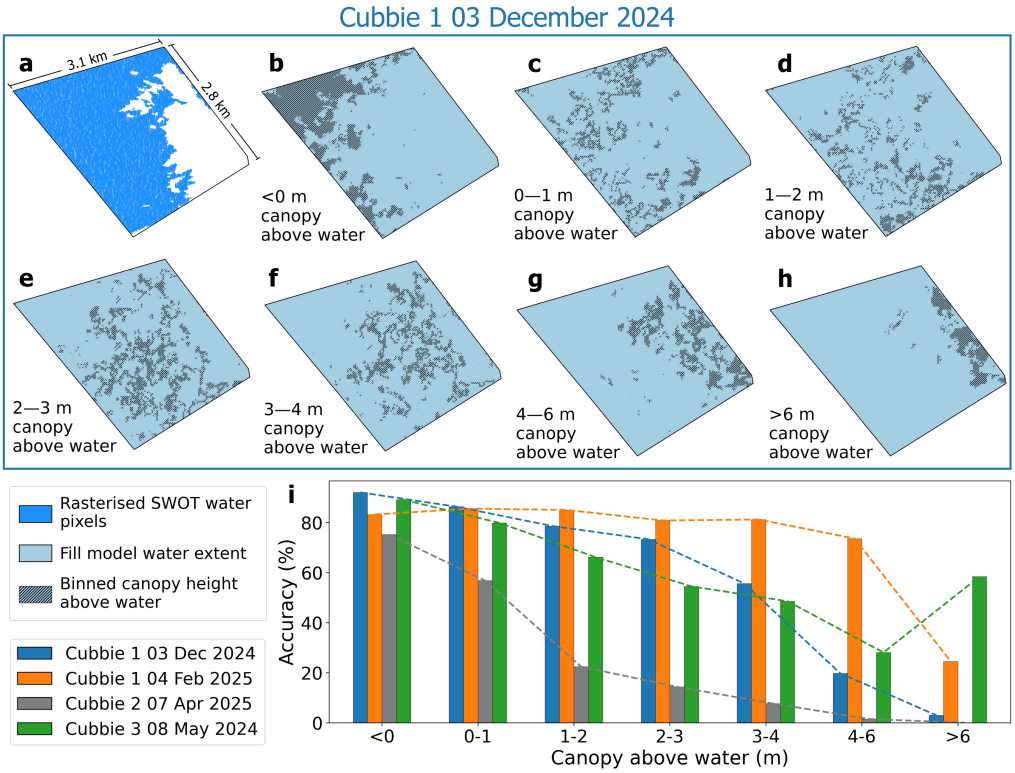


Figure 3.3: **(a)** Rasterised SWOT water-classified pixels and **(b-h)** spatial plots of the simulated water extent and canopy height above the water surface binned into pixels with <0, 1-2, 2-3, 3-4, 4-6 and >6 m of canopy above the water, for Cubbie 1, on 03 December 2024. **(i)** The SWOT water detection accuracy based on the binned canopy height above the water pixels, for a subset of dams and epochs.

Figures 3.4a and 3.4e show two transects (arrows in Figures 3.4b and 3.4f) over dams when the fill models showed that both dams should have been entirely covered in water (Figures 3.4d and 3.4h). However, substantial areas of both dams were misclassified by SWOT as non-water (Figures 3.4b and 3.4f) due to low coherent power of the radar signal

(e.g. Cubbie 1 from ∼1700-2000 m and ∼2600-2900 m (Figure 3.4a)). In some cases, this loss was explained by the height of vegetation above the water, as seen in Cubbie 1 (Figures 3.4a-d). Here, the regions of relatively lower coherent power (∼< 70-75 dB) correlated with the regions where the canopy was higher above the water (>4 m) (Figures 3.4a and 3.4c).

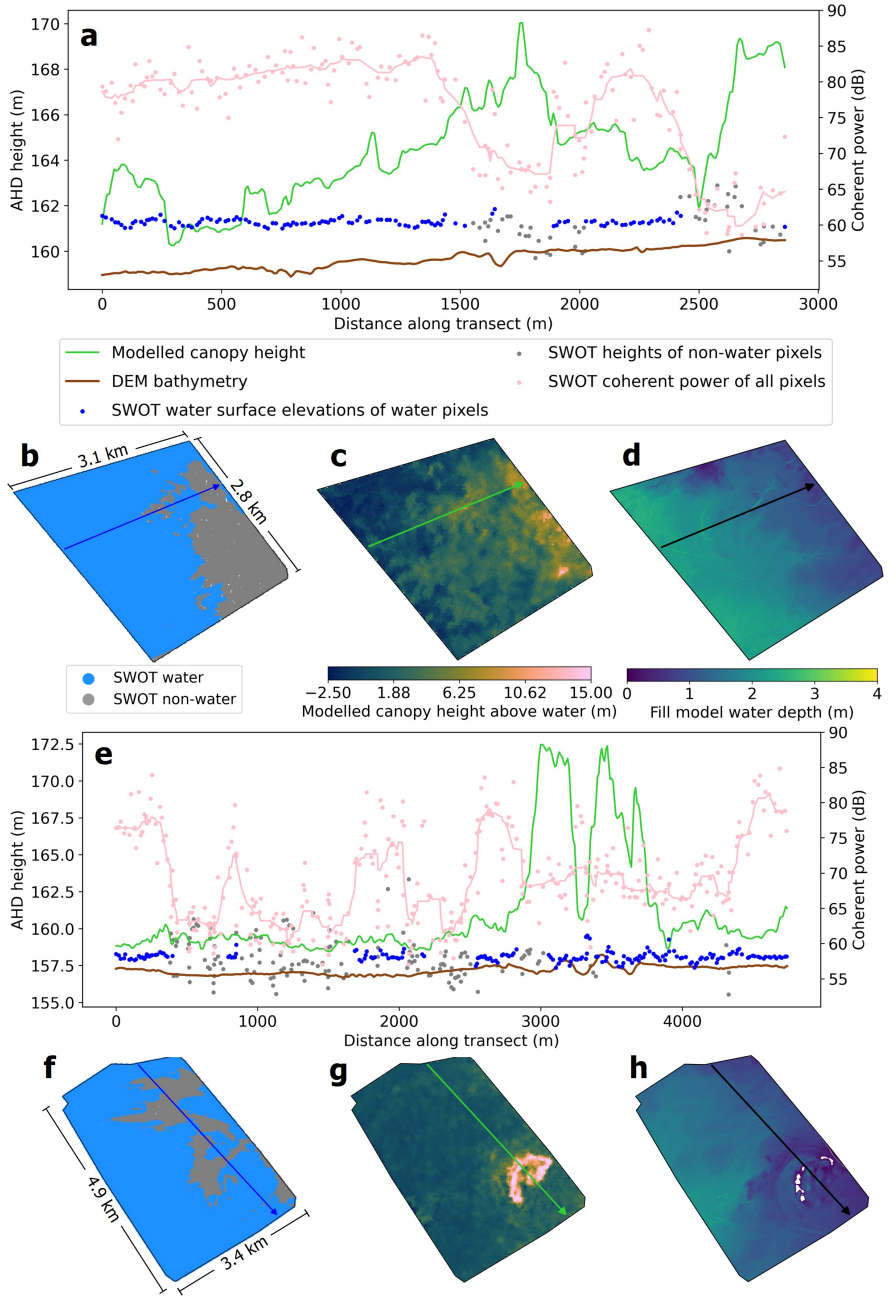


Figure 3.4: SWOT water detection compared to coherent power and canopy height. **(a)** Transect of AHD heights of SWOT pixels, SWOT coherent power, and modelled canopy height across Cubbie 1 on 03 December 2024 with plots of **(b)** SWOT water and non-water pixels, **(c)** modelled canopy height, and **(d)** fill model water depth. **(e)** Transect of AHD heights of SWOT pixels, SWOT coherent power, and modelled canopy height across Cubbie 3 on 08 May 2024 with plots of **(f)** SWOT water and non-water pixels, **(g)** modelled canopy height, and **(h)** fill model water depth.

Furthermore, emergent vegetation did not explain all the losses in coherent power in Cubbie 3 (Figures 3.4e-h). The northern region of the dam (from 400-1800 m along the transect) had less than ~2 m of canopy above the water, yet the majority was misclassified as land (Figures 3.4e and 3.4f). Conversely, the area in the south-eastern corner of the

dam had a substantially taller canopy above the water (Figures 3.4e and 3.4g), but SWOT correctly detected water underneath most of this canopy (Figures 3.4e and 3.4f).

3.6 Discussion

The classification of a SWOT pixel as water occurs when the coherent power of the pixel and its neighbouring pixels is sufficiently high, although this threshold varies from pixel to pixel (JPL D-109532, 2025). We found that the SWOT classification algorithm sometimes classified wet soil areas as water (Figure 3.2). While the coherent power over these areas was lower than over a standing water surface, likely due to increased roughness causing diffuse scattering (JPL D-109532, 2025), they were nevertheless classified as 'open water'. Therefore, the classification algorithm may be overly sensitive to soil moisture, a finding that agrees with previous research (Bonassies et al., 2026), suggesting that a higher coherent power threshold may be required so that wet soil pixels are not classified as 'water'.

Conversely, SWOT misclassified water-covered areas as non-water. In some cases, vegetation height explained the losses in coherent power that caused these misclassifications. However, along with canopy height, the ability of SAR systems to penetrate a canopy also depends on the canopy density (Gašparović & Klobučar, 2021). Preliminary tests found that KaRIn backscatter is sensitive to surface structural complexity in dense vegetation, which causes volume scattering of the signal and decreased backscatter to the sensor (Fayne et al., 2024). Unfortunately, the available LiDAR survey in our study site was conducted during a drought period in 2018, when there was substantially drier vegetation across the dams. Therefore, this dataset could not provide accurate measurements of vegetation structural complexity for 2024-2026. Nevertheless, given that KaRIn backscatter and coherent power decrease when surface roughness is very high (JPL D-109532, 2025; Bonassies et al., 2026), increased vegetation density may have contributed to the missed SWOT water detections across some of the dams. In wetlands, vegetation responds dynamically to changing hydrological conditions (M. Liu et al., 2024; Raulings et al., 2010), meaning vegetative impacts on SWOT water detection are likely time-varying and complex. Furthermore, SWOT KaRIn backscatter is sensitive to wind conditions and incidence angle (McQuillan et al., 2025; Fayne & Smith, 2023; Fayne et al., 2024), which can affect the downstream PIXC classification algorithm. At low incidence angles (0.5-1.5°), backscatter typically decreases with increasing wind speed, and at larger incidence angles (3.5-4.5°) backscatter increases with wind speed (McQuillan et al., 2025). With our SWOT data at an incidence angle of 3°, missed water detections may have occurred in low wind conditions, but detailed wind speed information was unavailable for our study site.

These limitations of the SWOT water detection will impact quantifications of SWOT-derived water extent, with implications in areas such as wetland lakes with emergent vegetation that may cause SWOT to misclassify the water as land (e.g. Figures 3.1d-f).

Conversely, the sensitivity of SWOT to soil moisture could cause an overestimation of water extent. This could provide an explanation for why Callaway et al. (2026) found higher water surface elevation anomalies on pixels around the edges of wetland water bodies.

That SWOT can detect soil moisture at all offers the opportunity to observe soil moisture across wetlands globally at a high spatial resolution (tens of metres), unlike other soil moisture satellite missions with spatial resolution in hundreds of metres or kilometres (Feng et al., 2026; Z.-L. Li et al., 2021; L. Li et al., 2021). This capability could be critical in smaller wetlands where ecosystems function despite relatively low water levels (Platt & Corrick, 1994).

The hydrological monitoring tools used in this study have advantages and disadvantages for monitoring complex wetland environments. The fill model accurately simulates water extent across gently sloping land surfaces; however, it requires an accurate DEM and a mean water level estimate from standing water SWOT pixels. It also may not accurately simulate water extent if receding water leaves behind puddles on the land surface. In a complex wetland system such as the Narran Lakes wetland (Figure 3.1), a more sophisticated water flow model, including an evapotranspiration component, would better simulate changes in water extent with changing water levels. While Sentinel-2 provides high spatial and temporal resolution, making it useful for monitoring water extent, it is ineffective in cloudy conditions and it cannot directly estimate water surface elevation. SWOT data can now provide this information (e.g. Figure 3.1c), but its ability to detect water may be compromised in vegetated environments. Therefore, a hybrid approach should be considered to integrate these remote sensing datasets.

3.7 Conclusion

This study assessed the water detection capabilities and limitations of the SWOT satellite in large farm dams in Australia. We identified cases of misclassification in the SWOT PIXC data, where wet soil was incorrectly identified as water, or water as land. In some cases, increased canopy height above the standing water surface correlated with missed water detections. However, canopy height above the water was an inconsistent indicator of SWOT water detection accuracy, suggesting that this interaction is complex and that other factors such as vegetation density and wind may also affect SWOT water detection.

Open Research Section

The SWOT Level 2 Water Mask Pixel Cloud Data Product is publicly available through NASA Earthdata at `https://search.earthdata.nasa.gov/search/granules?p=C3233944986-POCLOUD` (Surface Water Ocean Topography (SWOT), 2025). The Sentinel-2 Analysis Ready Surface Reflectance data are publicly available through Digital Earth Australia (Geoscience Australia, 2022a, 2022b, 2022c). LiDAR data across Australia are publicly

available through the Elvis Elevation and Depth platform `https://elevation.fsdf.org.au/`. The Annual vegetation height for Australia for 2019 to 2024 datasets are available through CSIRO at `https://data.csiro.au/collection/csiro:66385` (Ticehurst & Newnham, 2024). The Python code developed in this study is available on Zenodo at (Taib & Tregoning, 2026a).

Chapter 4

Supporting information for manuscript

This chapter contains the Supporting Information document for the manuscript in Chapter 3. I made the following contributions to this chapter:

- Wrote the text and created all the figures

Introduction

Section 4.1 describes the process of obtaining cloud-masked Sentinel-2 data, and calculating the Modified Normalised Difference Water Index (MNDWI).

Section 4.2 describes the calculation of the Tasseled Cap Wetness (TCW) index, an alternative water index to the MNDWI that has also been used for water detection in wetlands.

Section 4.3 describes the process of assessing the similarity between fill model water extents and water extents obtained using the MNDWI or TCW index at different thresholds, using the Jaccard index.

Section 4.4 describes the process of calculating and plotting the transects of the DEM and canopy height rasters, and the SWOT pixel heights and coherent power along the transects, in Figure 3.2 and 3.4.

Section 4.5 describes the process of approximating the SWOT PIXC pixel points as polygons and rasterising these.

Figure 4.1 presents a map of the farm dams assessed in this study.

Figure 4.2 presents the accuracy assessment between the thresholded MNDWI water extents and the fill model water extents for epochs when dams were partially full.

Figure 4.3 presents the accuracy assessment between the thresholded TCW index water extents and the fill model water extents for epochs when dams were partially full.

4.1 Sentinel-2 data and Modified Normalised Difference Water Index (MNDWI)

We obtained freely available, analysis-ready Sentinel-2 images over the farm dams every 2-3 days from the Digital Earth Australia platform (Geoscience Australia, 2022a, 2022b,

2022c). We retained clear pixels using the 's2cloudlessmask' layer, which is a binary cloud mask derived from Sentinel Hub's machine learning cloud detection algorithm. We additionally filtered out epochs with >20% cloud cover over each image of the study region to retain only high quality images.

We then calculated the MNDWI:

$$MNDWI = \frac{\rho_{green} - \rho_{SWIR}}{\rho_{green} + \rho_{SWIR}} \tag{4.1}$$

where ρ_{green} is the surface reflectance in the green band (Sentinel-2 Band 3) and ρ_{SWIR} is the surface reflectance in the shortwave-infrared band (Sentinel-2 Band 11).

4.2 Description of the Tasseled Cap Wetness (TCW) index

The use of the Tasseled Cap Wetness (TCW) index (Crist, 1985) with a threshold of -0.035 has led to improved detection of water under flooded wetland vegetation in the Murray-Darling Basin (Dunn et al., 2019; Ticehurst et al., 2022). We used the coefficients derived by Shi and Xu (2019) for the TCW index applied using Sentinel-2 surface reflectance bands, calculated as:

$$\begin{aligned} TCW = {} & 0.2578\,\rho_{blue} + 0.2305\,\rho_{green} + 0.0883\,\rho_{red} + 0.1071\,\rho_{NIR} \\ & - 0.7611\,\rho_{SWIR1} - 0.5308\,\rho_{SWIR2} \end{aligned} \tag{4.2}$$

where ρ_{blue}, ρ_{green}, ρ_{red}, ρ_{NIR}, ρ_{SWIR1} and ρ_{SWIR2} are the Sentinel-2 surface reflectance values in the blue, green, red, near-infrared, shortwave-infrared 1 and shortwave-infrared 2 bands (Sentinel-2 bands 2, 3, 4, 8, 11 and 12, respectively). The surface reflectance values should be normalised to between 0.0 and 1.0 before calculating the TCW index.

We calculated the TCW index from Sentinel-2 data for epochs with partially filled dams that had a SWOT pass on the same day, and applied a range of thresholds (between -0.14 and 0.055). We then assessed the similarity of each of the thresholded TCW index water extents and the fill model water extents, as described in Section 4.3.

4.3 Similarity assessment of fill model water extents and Sentinel-2 water extents

We calculated the Jaccard index (Jaccard, 1901) to assess the similarity of each reference fill model extent raster and each thresholded MNDWI or TCW index raster. The Jaccard index summarises the similarity of water-classified areas in both rasters without considering correctly classified non-water areas, which could over-inflate the value in certain cases. This metric has been preferentially used for comparing water extent rasters (Kavats et al., 2022; Bonassies et al., 2026; Masoumi & Tourian, 2026). The Jaccard index is calculated:

$$Jaccard\ index = \frac{N_{True\ Positive}}{N_{True\ Positive} + N_{False\ Positive} + N_{False\ Negative}} \tag{4.3}$$

where $N_{True\ Positive}$ is the number of pixels classified as water in both rasters, $N_{False\ Positive}$ is the number of pixels classified as water in the MNDWI raster but not in the fill model raster, and $N_{False\ Negative}$ is the number of pixels classified as non-water in the MNDWI raster but as water in the fill model raster.

Figure 4.2 shows the Jaccard index between the fill model water extent rasters and the MNDWI water extent rasters with different MNDWI thresholds, for the epochs when the dams were partially filled and when SWOT and Sentinel-2 data were available on the same days. Generally, the thresholds that yielded the optimal Jaccard index (marked with stars on Figure 4.2a) were between -0.3 and 0. Figures 4.2b-e show the spatial water extents for Cubbie 1 on 25 February 2025, where the optimal MNDWI threshold of -0.35 (Figure 4.2d) yields high similarity (Jaccard index = 0.9) with the fill model water extent (Figure 4.2b). In contrast, a threshold that is too low overestimates the water extent (Figure 4.2c) and a threshold that is too high underestimates the water extent (Figure 4.2e). Figures 4.2f-i show the same water extent rasters but for Cubbie 5 on 17 March 2025, with an optimal MNDWI threshold of -0.3.

Figure 4.3 shows the same information as Figure 4.2 but using the TCW index instead of the MNDWI. The range of optimal thresholds (marked with stars on Figure 4.3a) was generally between -0.03 and -0.13. Three epochs (green, brown and purple lines in Figure 4.3a) had optimal thresholds on the lower end of the range used in the literature (between -0.035 and 0 (Crist, 1985; L. Li et al., 2021; Dunn et al., 2019)). However, other epochs had optimal threshold values lower than this range, down to ∼-0.13. Similarly to the MNDWI accuracy assessment, the epochs in which receding water formed puddles of water detected by the TCW index (light blue, grey, pink and orange epochs in Figure 4.3a) had low similarity to the modelled water extents. Figures 4.3b-e and 4.3f-i show spatial water extents for Cubbie 1 on 25 February 2025 and Cubbie 5 on 17 March 2025 respectively, from the fill model (Figures 4.3b, 4.3f), and the TCW index with optimal (Figures 4.3d, S3h) and suboptimal thresholds (Figures 4.3c, 4.3e, 4.3g, 4.3i) that under- or over-estimate the water extent.

4.4 Plotting of DEM and canopy height raster transects and SWOT pixel transects

We generated transects along the DEM and canopy height rasters by averaging each of the raster pixel values within 10 m radius circular regions every 10 m along the transect line. For the SWOT PIXC pixels, we selected and plotted the water surface elevations and coherent power of pixels within 10 m of the transect line. We additionally calculated and plotted the running median of the coherent power every 10 m using the selected SWOT pixels.

4.5 Rasterisation of SWOT pixels

Pixels must be aligned to a common grid and resolution to enable comparisons between different spatial datasets. To compare the SWOT PIXC water extent with other rasters, several approaches have been used. Bonassies et al. (2026) gridded the SWOT PIXC data at 10 m resolution to achieve a raster dataset comparable to Sentinel-2 derived water masks, but this approach smooths out the SWOT pixel footprints, resulting in a loss of the original precision of the PIXC data (Bonassies et al., 2026). Alternatively, Sales et al. (2025) compared the coordinates of the SWOT pixel centres to the corresponding pixel of other raster water masks, but this may introduce inconsistencies due to the different spatial footprints of the pixels of both datasets.

We instead approximated the SWOT pixel points as rectangular polygons with dimensions of ∼22 m in the along-track direction (Jet Propulsion Laboratory, 2025) and cross-track dimensions calculated based on the pixel areas provided in the PIXC data. We then rasterised these polygons onto the same 1 m grid as the binned canopy height rasters to facilitate a pixel-by-pixel raster analysis between the SWOT water extent and the canopy height above the water surface, as described in Section 3.5.

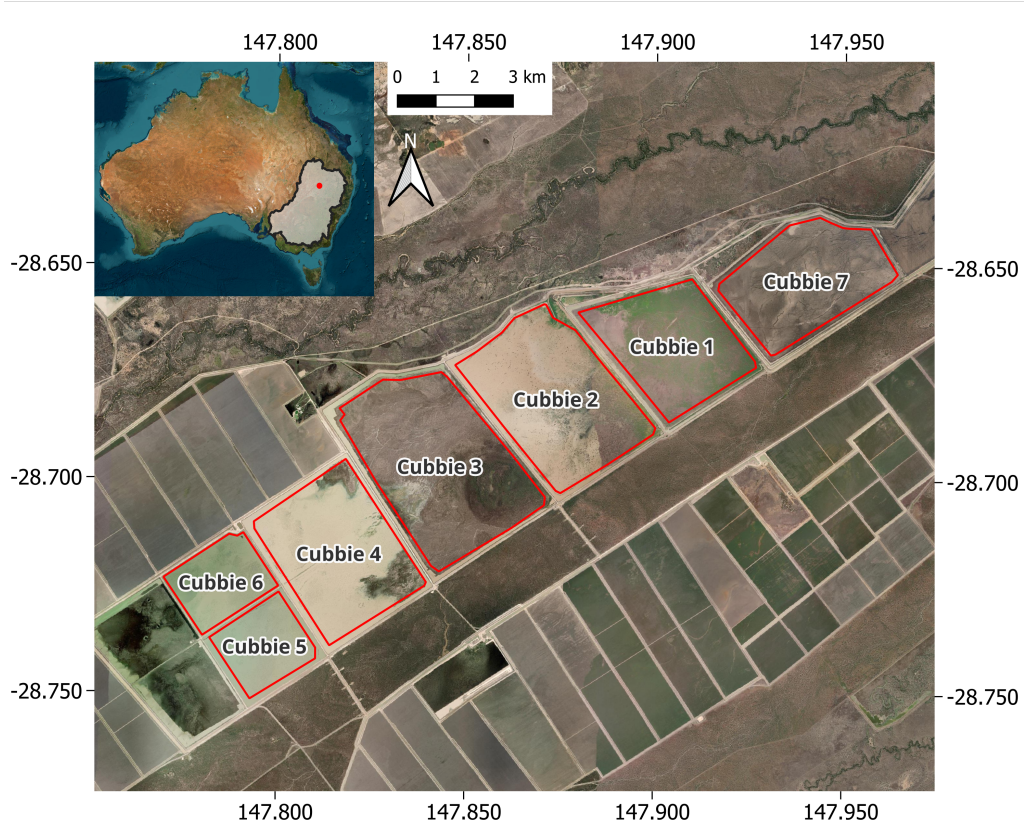


Figure 4.1: Location of the farm dams (red) on Cubbie Station in the Murray-Darling Basin, Australia (grey polygon in the inset map).

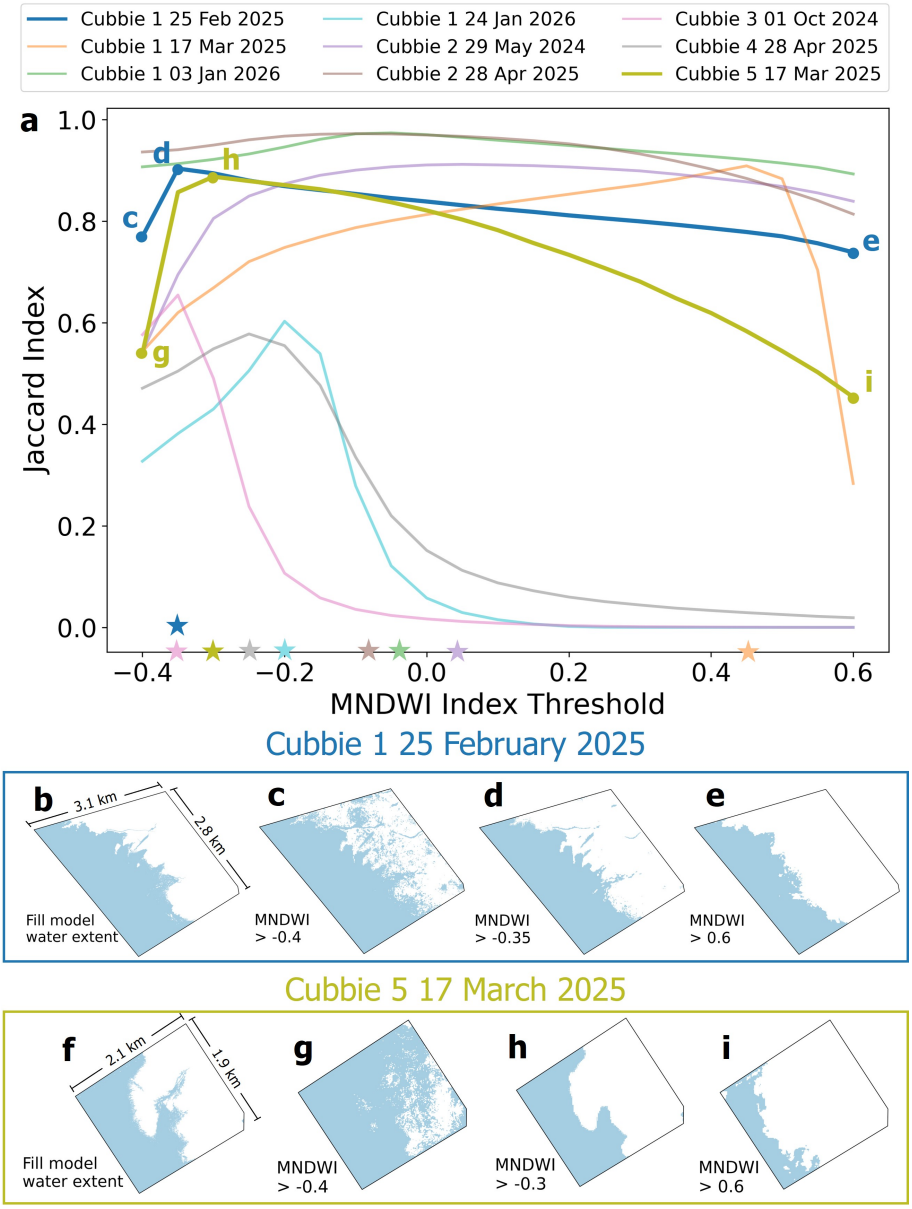


Figure 4.2: **(a)** Jaccard index between the fill model water extents and the water extents from the MNDWI at different thresholds for two partially-full dams at various epochs. The optimal MNDWI thresholds are marked with coloured stars. Spatial water extents for Cubbie 1 on 25 February 2025 from **(b)** the fill model, **(c and e)** the MNDWI with suboptimal thresholds, and **(d)** the MNDWI with optimal threshold (-0.35). Spatial water extents for Cubbie 5 on 17 March 2025 from **(f)** the fill model, **(g and i)** the MNDWI with suboptimal thresholds, and **(h)** the MNDWI with optimal threshold (-0.3). Letters in **(a)** relate to the spatial maps below.

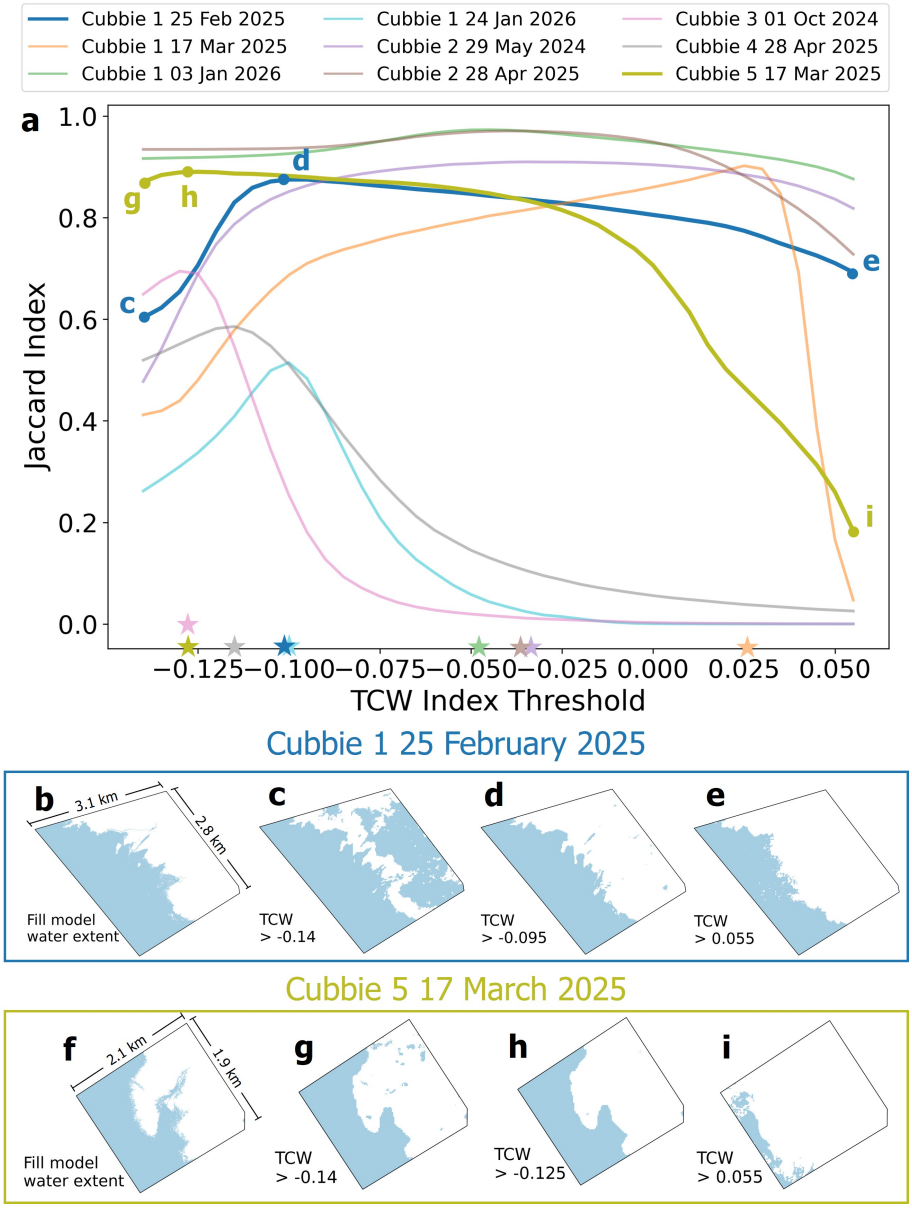


Figure 4.3: **(a)** Jaccard index between the fill model water extents and the water extents from the TCW index at different thresholds for two partially-full dams at various epochs. The optimal TCW index thresholds are marked with coloured stars. Spatial water extents for Cubbie 1 on 25 February 2025 from **(b)** the fill model, **(c and e)** the TCW index with suboptimal thresholds, and **(d)** the TCW index with optimal threshold (-0.095). Spatial water extents for Cubbie 5 on 17 March 2025 from **(f)** the fill model, **(g and i)** the TCW index with suboptimal thresholds, and **(h)** the TCW index with optimal threshold (-0.125). Letters in **(a)** relate to the spatial maps below.

Chapter 5

Discussion and conclusions

In this chapter, I discuss several limitations of my study and the implications of my findings. This includes implications for both the SWOT algorithm development team and for end-users of SWOT water extent or water surface elevation data in wetlands. I then present the overall conclusions of my thesis.

5.1 Limitations of this study

5.1.1 Datasets

One of the limitations of this study was the lack of in situ water extent data in the dams. In situ observations of water extent would provide a ground truth against which to validate the fill model water extents, and to identify the optimal Sentinel-2 water index and threshold for delineating water in this study site. As discussed in Section 3.6, the unavailability of recent LiDAR data was another limitation of my study, as there was no available information about the vegetation density across the dams during the study period. Furthermore, there are inherent limitations to the use of the annual vegetation height dataset I used. The coarse 30 m resolution of the dataset may 'smooth out' true variations in vegetation height that occur on a sub-pixel scale, even though these variations likely influence the coherent power received from a SWOT pixel. Therefore, the acquisition of recent LiDAR data over the study site would provide a more temporally consistent and accurate dataset of vegetation structural characteristics. Furthermore, given that the interaction between wind speed and incidence angle has been found to impact SWOT backscatter (as discussed in Section 2.3.2), it would be valuable to assess these impacts, provided wind speed data can be obtained from in situ or modelled observations, for a study site where SWOT observations at a range of incidence angles are available.

5.1.2 Raster-based analysis

The raster-based comparisons I conducted in Section 3.3 and Section 3.5 contain inherent uncertainties resulting from the different spatial resolutions of the input datasets. For example, the fill model water extents derived from the airborne LiDAR survey have a spatial resolution of 1 m. On the other hand, the Sentinel-2 MNDWI and TCW index water extent rasters have a native spatial resolution of 20 m. I chose to retain the 1 m resolution of the fill model as it is critical for accurately representing in detail the spread of

water across the dams. However, this may impact the pixel-by-pixel similarity calculation between the fill model extents and the Sentinel-2 extents, as the coarser Sentinel-2 dataset does not capture the small-scale variations in water extent that the model can capture. An alternative approach could be to coarsen the fill model extents to 20 m pixels (either by coarsening the input DEM or aggregating the output water extent), but this would introduce new uncertainty and result in a loss of the spatial detail of the modelled extents.

More generally, it should be noted that there are inherent limits to accurately representing reality using raw vector and raster data. Specifically, the ability of satellite sensors such as SWOT and Sentinel-2 to accurately delineate small-scale variations in water extent across heterogeneous landscapes is fundamentally constrained by the size of the raw pixels provided in each dataset. As discussed in Section 2.1, wetlands contain areas of mixed land cover, often on spatial scales smaller than the native resolution of satellite remote sensing systems. However, my analysis does not consider these sub-pixel variations. It instead assumes that each SWOT or Sentinel-2 pixel represents a homogeneous area of water or land. While this assumption does not reflect the reality of mixed wetland pixels, it is suitable for comparisons between SWOT and Sentinel-2 detected water extents, at a farm dam-scale.

5.2 Improving the SWOT PIXC data product

The misclassification issues I identified provide important information for SWOT algorithm developers. Identifying the physical conditions in which classification issues may occur could inform how the underlying SWOT classification algorithm could be modified to address such issues. For example, the process of assigning pixels to one of the 'low-coherence' water classes could be improved to include cases where vegetated water pixels with lower coherent power were incorrectly identified as 'land'. In my study, I found very few instances of pixels classified as 'low-coherence' across the dams, even though I identified water areas with lower coherent power that correlated with vegetation effects. Rather, these water areas were incorrectly classified as 'land' or 'land near water', suggesting that the built-in pixel classification may be too strict when classifying pixels in vegetated water surfaces that may have lower coherent power. While these pixels likely have less accurate water surface elevation estimates than true water-classified pixels, classifying them as 'low-coherence' water would aid end-users to easily identify these pixels as water and avoid underestimating the extent of a water body.

In order to identify regions where SWOT may be prone to misclassification issues, the PIXC data could include a new pixel quality flag that identifies global wetland areas. For example, the PIXC data already includes a 'prior water' mask, which delineates areas that are likely to be open water according to independent global surface water datasets (SWOT-IS-CDM-1447-CNES, Revision B, 2024). A similar mask could be developed for wetlands, and used to flag wetland areas that may contain the misclassification issues identified in my study. Similarly, Desrochers et al. (2021) has proposed that an additional quality

flag could be added to identify pixels containing emergent riparian vegetation, using a new global high resolution map of emergent vegetation that could be developed (Klemas, 2013; Huylenbroeck et al., 2020). A 'wetland' or 'emergent vegetation' flag would help alert end-users of SWOT pixels with potentially inaccurate classifications, which would be particularly useful in larger-scale regional or global applications of SWOT data.

5.3 Implications for wetland monitoring

5.3.1 Improving SWOT water extent retrievals

End-users of SWOT data in wetlands should be aware of the potential misclassification risks in vegetated areas and wet soils, and should not rely solely on SWOT data in its current form for quantifying wetland water extents (Shirafkan et al., 2026; Bhattarai et al., 2026; Normandin et al., 2026; Taib & Tregoning, 2026b). Rather, post-processing methods can be explored to improve SWOT water extents, as well as the combination of SWOT and other satellite datasets.

Shirafkan et al. (2026) developed three machine learning models to integrate SWOT PIXC variables and a global water occurrence dataset to improve the water extents over small reservoirs from the PIXC and spatial products. They concluded that post-processing machine learning-based approaches can help to compensate for water detection inaccuracies in SWOT data in littoral zones and across the surface of a reservoir where SWOT returns may have been noisy. However, they highlight that the effectiveness of these approaches may vary in more hydrologically complex environments such as wetlands (Shirafkan et al., 2026). This would be a useful avenue for future studies, especially given the promising results of Shirafkan et al. (2026) over small water bodies.

Another promising method to complement the water extents from SWOT is to integrate SWOT with other satellite data. For example, optical satellite data in many cases yields improved water delineation compared to SWOT (as shown in Fig. 3.1 and in Bhattarai et al. (2026), Girard et al. (2025) and Rai et al. (2026a)). However, this is subject to the limitations of optical systems, (see Section 2.3.1) including constrained spatial coverage due to cloud cover, and potential water detection inaccuracies in mixed land covers. More importantly, the potential for developing hybrid approaches to combine SWOT, optical data and SAR data is immense, and would enable analysts to leverage the unique capabilities of each approach. In particular, SAR data has been used for mapping wetland inundation as it is not limited by cloud cover (Hess et al., 1995; Grimaldi et al., 2020; Kasischke et al., 2003; Mitchell et al., 2015). To address the low spatial and temporal resolution of SAR data, it can be merged with optical data to improve inundation extent mapping (Gašparović & Klobučar, 2021; Y. Liu et al., 2026). These datasets could then complement the SWOT water extents, by providing improved water detection over open vegetated water surfaces where SWOT may underestimate water extents.

As described in Section 3.6, the SWOT misclassification of wet soil as 'open water' may cause an overestimation of water extent in wetlands. This further necessitates the

use of other datasets to validate the water extents detected by SWOT. However, existing satellite soil moisture missions only provide medium or coarse spatial resolution observations (i.e. hundreds of metres or kilometres), which are insufficient to validate the SWOT wet soil detections. Therefore, I recommend that end users assess SWOT water extents in conjunction with high resolution optical satellite data such as Sentinel-2 data, which would help determine where SWOT water observations are unlikely to be open water surfaces (e.g. in the case shown in Figure 3.2a-c).

5.3.2 Implications for SWOT water surface elevation retrievals

As discussed in Section 2.3.2, the standard filtering of PIXC data generally involves the selection of only water-classified pixels, meaning that inaccuracies in the PIXC classification will propagate into the water surface elevation estimates retained for subsequent analyses.

Section 3.2 highlights how this issue can result in an inaccurate mean water surface elevation if wet soil pixels are aggregated with true open water pixels. My method of utilising only High Coherent Power (HCP) SWOT pixels in the mean surface elevation estimate over a water body helps minimise contamination from potential wet soil pixels in the littoral zone. This is important for accurate quantifications of water storage within wetland water bodies (Callaway et al., 2026).

On the other hand, SWOT misclassifications of water areas as non-water will need further attention. In cases where a flat water body has gaps from pixels misclassified as 'land' (e.g. Figure 3.4), the water surface elevations of the missing pixels could be interpolated using the water surface elevations of the surrounding correctly classified water pixels. However, cases where SWOT may misclassify pixels across an entire water body as 'land' (e.g. in the channelised floodplain area of the Narran Lakes wetland in Figure 3.1) are more complicated. This is because pixels classified as 'land' typically have less accurate height estimates than water-classified pixels, as they have lower coherent power (e.g. heights of grey, non-water pixels in Figures 3.2 and 3.4). However, it is possible that some 'land' pixels with relatively higher coherent power could yield usable height estimates. While beyond the scope of this thesis, a method could be developed to filter and validate these pixels to obtain acceptable water surface elevation estimates for pixels that were incorrectly classified as non-water.

5.4 Conclusions

The ability to accurately and consistently monitor the Earth's surface waters is critical for quantifying changes in the availability of water in freshwater environments. A variety of monitoring tools exist that each provide unique information on hydrological dynamics within the world's wetlands. The new SWOT satellite mission has been helping to address important gaps in our current knowledge of inland water levels and depths, but uncertainties remain about the ability of this satellite to detect water in wetlands. In

this thesis, I have investigated the capability of the SWOT satellite for detecting water in vegetated, temporarily inundated farm dams in Australia. I found that wetland surface characteristics such as soil moisture and emergent vegetation were dominant controls on the ability of SWOT to detect water accurately. I identified cases where SWOT incorrectly detected wet soil as open water. In some cases, taller emergent vegetation was linked to lower coherent power received from the water surface, causing misclassifications of water areas as non-water. However, this relationship was inconsistent, suggesting that there is nevertheless substantial value in utilising SWOT for detecting water in environments such as inundated woody vegetation (e.g. Fig. 3.4e-h), particularly given that existing optical satellite systems may be inadequate in these conditions (Salameh et al., 2026). Furthermore, my GIS-based fill model demonstrates the new value of SWOT water surface elevation measurements for modelling water extents and depths across wetlands, provided an accurate DEM is available. This motivates further efforts to embed SWOT data within hydrodynamic wetland and floodplain modelling. In combination with additional sources of water extent data such as optical and SAR satellite data, the hydrological insights provided by the SWOT satellite mission will help inform the management of freshwater environments and water resources globally.

References

Anokye, M., & Hashemi-Beni, L. (2026). Integrating LiDAR and multispectral remote sensing data for understanding wetland-flood dynamics: a literature review. *Frontiers in Environmental Science*, *14*, 1757715. doi: 10.3389/fenvs.2026.1757715

Armstrong, R., Kayter, C., Shook, K., & Hill, H. (2013). Using the Wetland DEM Ponding Model as a Diagnostic Tool for Prairie Flood Hazard Assessment. In *Putting prediction in ungauged basins into practice* (p. 255-270). Canadian Water Resources Association.

Arthur, A. D., Reid, J. R. W., Kingsford, R. T., Mcginness, H. M., Ward, K. A., & Harper, M. J. (2012). Breeding flow thresholds of colonial breeding waterbirds in the Murray-Darling Basin, Australia. *Wetlands*, *32*(2), 257–265. doi: 10.1007/s13157-011-0235-y

Baggio, G., Qadir, M., & Smakhtin, V. (2021). Freshwater availability status across countries for human and ecosystem needs. *Science of The Total Environment*, *792*, 148230. doi: 10.1016/j.scitotenv.2021.148230

Beltrão, D., Cicerelli, R. E., Lappicy, T., Sales, L. O., Teixeira, A. D. A., Cunha, L. S. D., ... Almeida, T. D. (2026). SWOT: Reviewing Challenges and Opportunities in Hydrological Applications to Inland Waters. *IEEE Access*, *14*, 77225–77238. doi: 10.1109/ACCESS.2026.3690929

Bhattarai, T. N., Aryal, S., Pokhrel, Y., & Pandey, V. P. (2026). SWOT versus legacy satellite missions: assessing water surface elevation and surface water extent in complex river settings. *Geocarto International*, *41*(1), 2679903. doi: 10.1080/10106049.2026.2679903

Biancamaria, S., Lettenmaier, D., Pevelsky, T., & Young, N. (2016). The SWOT mission and its capabilities for land hydrology. *Remote sensing and water resources*, *37*, 307-337. doi: 10.1007/9783319324494_6

Bino, G., Steinfeld, C., & Kingsford, R. T. (2014). Maximizing colonial waterbirds' breeding events using identified ecological thresholds and environmental flow management. *Ecological Applications*, *24*(1), 142–157. doi: 10.1890/13-0202.1

Bonassies, Q., Fatras, C., Peña-Luque, S., Dubois, P., Piacentini, A., Cassan, L., ... Nguyen, T. H. (2026). A comprehensive study of Surface Water and Ocean Topography (SWOT) Pixel Cloud data for flood extent extraction. *Remote Sensing of Environment*, *333*, 115101. doi: 10.1016/j.rse.2025.115101

Bourgeau-Chavez, L. L., Riordan, K., Powell, R. B., Miller, N., & Nowels, M. (2009). Improving wetland characterization with multi-sensor, multi-temporal SAR and optical/infrared data fusion. In *Advances in geoscience and remote sensing.* IntechOpen. doi: 10.5772/8327

Brandis, K. J., Kingsford, R. T., Ren, S., & Ramp, D. (2011). Crisis Water Management and Ibis Breeding at Narran Lakes in Arid Australia. *Environmental Management*, *48*(3), 489–498. doi: 10.1007/s00267-011-9705-5

Bullock, A., & Acreman, M. (2003). The role of wetlands in the hydrological cycle. *Hydrology and Earth System Sciences*, *7*(3), 358–389. doi: 10.5194/hess-7-358-2003

Bunn, S. E., & Arthington, A. H. (2002). Basic principles and ecological consequences of altered flow regimes for aquatic biodiversity. *Environmental Management*, *30*(4), 492–507. doi: 10.1007/s00267-002-2737-0

Callaway, M., Taib, M., Tregoning, P., Gouramanis, C., & Dodd, L. (2026). Surface Water and Ocean Topography satellite data reveals flood depths and environmental flows in wetlands. *Communications Earth & Environment*, *7*, 831. doi: 10.1038/s43247-026-03816-1

Capon, S. J., Stewart-Koster, B., & Bunn, S. E. (2021). Future of Freshwater Ecosystems in a 1.5°C Warmer World. *Frontiers in Environmental Science*, *9*, 784642. doi: 10.3389/fenvs.2021.784642

Cerbelaud, A., Wade, J., David, C. H., Durand, M., Frasson, R. P. M., Pavelsky, T., & Oubanas, H. (2026). Wide-swath altimetry maps bank shapes and storage changes in global rivers. *Nature*, *651*(8106), 666–671. doi: 10.1038/s41586-026-10218-y

Chandanpurkar, H. A., Famiglietti, J. S., Gopalan, K., Wiese, D. N., Wada, Y., Kakinuma, K., ... Zhang, F. (2025). Unprecedented continental drying, shrinking freshwater availability, and increasing land contributions to sea level rise. *Science Advances*, *11*(30), eadx0298. doi: 10.1126/sciadv.adx0298

Chandler, H. C., McLaughlin, D. L., & Haas, C. A. (2024). Informing the Conservation of Ephemerally Flooded Wetlands Using Hydrologic Regime and LiDAR-Based Habitat Assessments. *Wetlands*, *44*(3), 33. doi: 10.1007/s13157-023-01767-3

Che, L., Li, S., & Liu, X. (2025). Improved surface water mapping using satellite remote sensing imagery based on optimization of the Otsu threshold and effective selection of remote-sensing water index. *Journal of Hydrology*, *654*, 132771. doi: 10.1016/j.jhydrol.2025.132771

Chen, Y., Colloff, M. J., Lukasiewicz, A., & Pittock, J. (2020). A trickle, not a flood: environmental watering in the Murray–Darling Basin, Australia. *Marine and Freshwater Research*, *72*(5), 601–619. doi: 10.1071/MF20172

Cohen, S., Brakenridge, G. R., Kettner, A., Bates, B., Nelson, J., McDonald, R., ... Zhang, J. (2018). Estimating Floodwater Depths from Flood Inundation Maps and Topography. *JAWRA Journal of the American Water Resources Association*, *54*(4), 847–858. doi: 10.1111/1752-1688.12609

Convention on wetlands of international importance especially as waterfowl habitat. (1971). United Nations Treaty Series, Volume 996, p. 245. Retrieved from `https://www.unesco.org/en/legal-affairs/convention-wetlands-international-importance-especially-waterfowl-habitat` (Entered into force 21 December 1975)

Crist, E. P. (1985). A TM tasseled cap equivalent transformation for reflectance factor data. *Remote Sensing of Environment*, *17*(3), 301–306. doi: 10.1016/0034-4257(85)90102-6

De Paiva, R. C. D., Buarque, D. C., Collischonn, W., Bonnet, M., Frappart, F., Calmant, S., & Bulhões Mendes, C. A. (2013). Large-scale hydrologic and hydrodynamic modeling of the Amazon River basin. *Water Resources Research*, *49*(3), 1226–1243. doi: 10.1002/wrcr.20067

Department of Climate Change, Energy the Environment and Water. (2025). *Evaluation of wetland flow and connectivity objectives and targets: inundation* [Technical report supporting the NSW Basin Plan Matter 8 reporting 2019 to 2024]. Retrieved from `https://www.environment.nsw.gov.au/sites/default/files/2025-05/inundation-evaluation-of-wetland-flow-and-connectivity-250042.pdf`

Department of Environment, Climate Change and Water NSW. (2011). *NSW Rivers Environmental Restoration Program.* Retrieved from `https://www.environment.nsw.gov.au/sites/default/files/2024-10/rivers-environmental-restoration-project-final-report-110240.pdf`

Department of the Environment and Energy. (2015). *Australia's Ramsar Implementation Plan 2016-2018* [Implementation Plan for the First Triennium of the Ramsar Strategic Plan 2016-2024]. Retrieved from `https://www.agriculture.gov.au/sites/default/files/documents/australias-ramsar-implementation-plan-2016-18.pdf`

Desrochers, N., Trudel, M., Biancamaria, S., Siles, G., Desroches, D., Carbonne, D., & Leconte, R. (2021). Effects of aquatic and emergent riparian vegetation on SWOT mission capability in detecting surface water extent. *IEEE Journal of Selected Topics in Applied Earth Observations and Remote Sensing*, *14*, 12467–12478. doi: 10.1109/JSTARS.2021.3128133

Drusch, M., Del Bello, U., Carlier, S., Colin, O., Fernandez, V., Gascon, F., ... Bargellini, P. (2012). Sentinel-2: ESA's Optical High-Resolution Mission for GMES Operational Services. *Remote Sensing of Environment*, *120*, 25–36. doi: 10.1016/j.rse.2011.11.026

Du, Y., Zhang, Y., Ling, F., Wang, Q., Li, W., & Li, X. (2016). Water Bodies' Mapping from Sentinel-2 Imagery with Modified Normalized Difference Water Index at 10-m Spatial Resolution Produced by Sharpening the SWIR Band. *Remote Sensing*, *8*(4), 354. doi: 10.3390/rs8040354

Dunn, B., Lymburner, L., Newey, V., Hicks, A., & Carey, H. (2019). Developing a Tool for Wetland Characterization Using Fractional Cover, Tasseled Cap Wetness And Water Observations From Space. In *IGARSS 2019 - 2019 IEEE International Geoscience and Remote Sensing Symposium* (pp. 6095–6097). (ISSN: 2153-7003) doi: 10.1109/IGARSS.2019.8897806

Falkenmark, M., Wang-Erlandsson, L., & Rockström, J. (2019). Understanding of water resilience in the Anthropocene. *Journal of Hydrology X*, *2*, 100009. doi: 10.1016/j.hydroa.2018.100009

Fayne, J. V., & Smith, L. C. (2023). How does wind influence near-nadir and low-incidence ka-band radar backscatter and coherence from small inland water bodies? *Remote Sensing*, *15*(13), 3361. doi: 10.3390/rs15133361

Fayne, J. V., Smith, L. C., Liao, T.-H., Pitcher, L. H., Denbina, M., Chen, A. C., ... Williams, B. A. (2024). Characterizing near-nadir and low incidence ka-band SAR backscatter from wet surfaces and diverse land covers. *IEEE Journal of Selected Topics in Applied Earth Observations and Remote Sensing*, *17*, 985–1006. doi: 10.1109/JSTARS.2023.3317502

Feng, S., Li, A., Zhou, R., Butterbach-Bahl, K., Guan, K., Jin, Z., ... Wang, S. (2026). Global daily 9 km remotely sensed soil moisture (2015–2025) with microwave radiative transfer-guided learning. *Scientific Data*, *13*(1), 435. doi: 10.1038/s41597-026-06721-6

Feyisa, G. L., Meilby, H., Fensholt, R., & Proud, S. R. (2014). Automated water extraction index: A new technique for surface water mapping using landsat imagery. *Remote Sensing of Environment*, *140*, 23–35. doi: 10.1016/j.rse.2013.08.029

Fisher, A., Flood, N., & Danaher, T. (2016). Comparing Landsat water index methods for automated water classification in eastern Australia. *Remote Sensing of Environment*, *175*, 167–182. doi: 10.1016/j.rse.2015.12.055

Gallant, A. L. (2015). The challenges of remote monitoring of wetlands. *Remote Sensing*, *7*(8), 10938–10950. doi: 10.3390/rs70810938

Gašparović, M., & Klobučar, D. (2021). Mapping Floods in Lowland Forest Using Sentinel-1 and Sentinel-2 Data and an Object-Based Approach. *Forests*, *12*(5), 553. doi: 10.3390/f12050553

Geoscience Australia. (2022a). *Geoscience Australia Sentinel-2A MSI Analysis Ready Data Collection 3 - DEA Surface Reflectance (Sentinel-2A MSI).* doi: 10.26186/146552

Geoscience Australia. (2022b). *Geoscience Australia Sentinel-2B MSI Analysis Ready Data Collection 3 - DEA Surface Reflectance (Sentinel-2B MSI).* doi: 10.26186/146551

Geoscience Australia. (2022c). *Geoscience Australia Sentinel-2C MSI Analysis Ready Data Collection 3.* doi: 10.26186/150143

Gilvear, D. J., & Bradley, C. (2000). Hydrological monitoring and surveillance for wetland conservation and management; a UK perspective. *Physics and Chemistry of the Earth, Part B: Hydrology, Oceans and Atmosphere*, *25*(7), 571–588. doi: 10.1016/S1464-1909(00)00068-X

Girard, F., Kergoat, L., Ibrahim, M., Wubda, M., Nikiema, D., Abdourhamane Touré, A., ... Manuela, G. (2025, 01). Performance of the Surface Water and Ocean Topography (SWOT) Mission for monitoring small lakes in West Africa. *IEEE Journal of Selected Topics in Applied Earth Observations and Remote Sensing*, *18*, 14855-14869. doi: 10.1109/JSTARS.2025.3570859

Goulburn-Broken Catchment Management Authority. (2024). *Barmah Forest (Murray System) Seasonal Watering Proposal 2024-25.* Retrieved from `https://www.gbcma.vic.gov.au/downloads/Environmental_Water/Barmah%20_Forest_SWP_FINAL_2024_25.pdf`

Grimaldi, S., Xu, J., Li, Y., Pauwels, V., & Walker, J. (2020). Flood mapping under vegetation using single SAR acquisitions. *Remote Sensing of Environment*, *237*, 111582. doi: 10.1016/j.rse.2019.111582

Guo, M., Li, J., Sheng, C., Xu, J., & Wu, L. (2017). A Review of Wetland Remote Sensing. *Sensors*, *17*(4), 777. doi: 10.3390/s17040777

Günen, M. A., & Atasever, U. H. (2024). Remote sensing and monitoring of water resources: A comparative study of different indices and thresholding methods. *The Science of the Total Environment*, *926*, 172117. doi: 10.1016/j.scitotenv.2024.172117

Haag, K. H., Lee, T. M., & Herndon, D. C. (2005). Bathymetry and vegetation in isolated marsh and cypress wetlands in the northern Tampa Bay Area, 2000-2004. *Scientific Investigations Report*. (Number: 2005-5109) doi: 10.3133/sir20055109

Hart-Davis, M. G., Scherer, D., Schwatke, C., Sawyer, A. H., Pavelsky, T. M., Ray, R. D., ... Seitz, F. (2026). Observing the tidal pulse of rivers from wide-swath satellite altimetry. *Nature*, *652*(8109), 371–378. doi: 10.1038/s41586-026-10287-z

Heath, J. T., Grimmett, L., Gopalakrishnan, T., Thomas, R. F., & Lenehan, J. (2024). Integrating Sentinel 2 Imagery with High-Resolution Elevation Data for Automated Inundation Monitoring in Vegetated Floodplain Wetlands. *Remote Sensing*, *16*(13), 2434. doi: 10.3390/rs16132434

Hess, L., Melack, J., Filoso, S., & Yong Wang. (1995). Delineation of inundated area and vegetation along the Amazon floodplain with the SIR-C synthetic aperture radar. *IEEE Transactions on Geoscience and Remote Sensing*, *33*(4), 896–904. doi: 10.1109/36.406675

Hou, X., Feng, L., Dai, Y., Hu, C., Gibson, L., Tang, J., ... Zheng, C. (2022). Global mapping reveals increase in lacustrine algal blooms over the past decade. *Nature Geoscience*, *15*, 1–5. doi: 10.1038/s41561-021-00887-x

Huylenbroeck, L., Laslier, M., Dufour, S., Georges, B., Lejeune, P., & Michez, A. (2020). Using remote sensing to characterize riparian vegetation: A review of available tools and perspectives for managers. *Journal of Environmental Management*, *267*, 110652. doi: 10.1016/j.jenvman.2020.110652

Hyyppä, J., Hyyppä, H., Yu, X., Kaartinen, H., Kukko, A., & Holopainen, M. (2009). Forest Inventory Using Small-Footprint Airborne LiDAR. In *Topographic laser ranging and scanning.* CRC Press.

Jaccard, P. (1901). Distribution de la flore alpine dans le bassin des dranses et dans quelques régions voisines. *Bulletin de la Societe Vaudoise des Sciences Naturelles*, *37*(140), 547-579. doi: 10.5169/SEALS-266440

Jackson, C. R., Thompson, J. A., & Kolka, R. (2014). Wetland soils, hydrology and geomorphology. In D. Batzer & R. Sharitz (Eds.), *Ecology of freshwater and estuarine wetlands* (pp. 23–60). University of California Press.

Jet Propulsion Laboratory. (2025). *JPL D-56411, Revision C, SWOT Product Description Document: Level 2 KaRIn High Rate Water Mask Pixel Cloud (L2_HR_PIXC) Data Product.* Jet Propulsion Laboratory Internal Document.

JPL D-105504. (2023). *SWOT Algorithm Theoretical Basis Document: Level 2 KaRIn High Rate Pixel Cloud (L2_HR_PIXC) Science Algorithm Software.* Retrieved from `https://archive.podaac.earthdata.nasa.gov/podaac-ops-cumulus-docs/web-misc/swot_mission_docs/atbd/D-105504_SWOT_ATBD_L2_HR_PIXC_20230713a_cite2.pdf`

JPL D-109532. (2025). *SWOT Science Data Products User Handbook* (Vol. Revision A). Jet Propulsion Laboratory Internal Document, Pasadena, CA.

Karami, A., Baghdadi, N., Turki, M.-D., Bazzi, H., Cazals, C., Oubanas, H., ... Gasnier, N. (2026). Monitoring small water bodies using SWOT PIXC water level data; insight from On-farm reservoirs. *Remote Sensing Applications: Society and Environment*, *43*, 102209. doi: 10.1016/j.rsase.2026.102209

Karim, F., Kim, S., Ticehurst, C., Hughes, J., Marvanek, S., Gibbs, M., ... Petheram, C. (2024). *Floodplain inundation mapping and modelling for the Victoria catch-*

ment. Retrieved 2026-09-20, from `https://publications.csiro.au/publications/publication/PIcsiro:EP2024-3280` doi: 10.25919/SCYR-Z414

Kasischke, E. S., Smith, K. B., Bourgeau-Chavez, L. L., Romanowicz, E. A., Brunzell, S., & Richardson, C. J. (2003). Effects of seasonal hydrologic patterns in south Florida wetlands on radar backscatter measured from ERS-2 SAR imagery. *Remote Sensing of Environment*, *88*(4), 423–441. doi: 10.1016/j.rse.2003.08.016

Kavats, O., Khramov, D., & Sergieieva, K. (2022). Surface water mapping from SAR images using optimal threshold selection method and reference water mask. *Water*, *14*(24), 4030. doi: 10.3390/w14244030

Kica, S., Pavelsky, T. M., Fayne, J. V., & Williams, B. A. (2025). SWOT Water Surface Elevation in Herbaceous Wetlands of Florida's Everglades. *Geophysical Research Letters*, *52*(9), e2025GL114956. doi: https://doi.org/10.1029/2025GL114956

Kingsford, R. (2000). Ecological impacts of dams, water diversions and river management on floodplain wetlands in Australia. *Austral Ecology*, *25*(2), 109-127. doi: 10.1046/j.1442-9993.2000.01036.x

Klemas, V. (2013). Remote sensing of emergent and submerged wetlands: an overview. *International Journal of Remote Sensing*, *34*(18), 6286–6320. doi: 10.1080/01431161.2013.800656

Kordelas, G. A., Manakos, I., Lefebvre, G., & Poulin, B. (2019). Automatic Inundation Mapping Using Sentinel-2 Data Applicable to Both Camargue and Doñana Biosphere Reserves. *Remote Sensing*, *11*(19), 2251. doi: 10.3390/rs11192251

Kreibich, J., Bino, G., Zheng, H., Chiew, F., Glamore, W., Woods, J., & Kingsford, R. T. (2024). River regulation and climate change reduce river flows to major Australian floodplain wetland. *Journal of Environmental Management*, *370*, 122962. doi: 10.1016/j.jenvman.2024.122962

Lang, M. W., Townsend, P. A., & Kasischke, E. S. (2008). Influence of incidence angle on detecting flooded forests using C-HH synthetic aperture radar data. *Remote Sensing of Environment*, *112*(10), 3898–3907. doi: 10.1016/j.rse.2008.06.013

Leblanc, M., Tweed, S., Van Dijk, A., & Timbal, B. (2021). A review of historic and future hydrological changes in the Murray-Darling Basin. *Global and Planetary Change*, *80-81*, 226–246. doi: 10.1016/j.gloplacha.2011.10.012

Lefebvre, G., Davranche, A., Willm, L., Campagna, J., Redmond, L., Merle, C., ... Poulin, B. (2019). Introducing WIW for Detecting the Presence of Water in Wetlands with Landsat and Sentinel Satellites. *Remote Sensing*, *11*(19), 2210. doi: 10.3390/rs11192210

Lehner, B., Anand, M., Fluet-Chouinard, E., Tan, F., Aires, F., Allen, G. H., ... Thieme, M. (2025). Mapping the world's inland surface waters: an upgrade to the Global Lakes and Wetlands Database (GLWD v2). *Earth System Science Data*, *17*(6), 2277-2329. doi: 10.5194/essd-17-2277-2025

Li, L., Su, H., Du, Q., & Wu, T. (2021). A novel surface water index using local background information for long term and large-scale Landsat images. *ISPRS Journal of Photogrammetry and Remote Sensing*, *172*, 59-78. doi: 10.1016/j.isprsjprs.2020.12.003

Li, Z.-L., Leng, P., Zhou, C., Chen, K.-S., Zhou, F.-C., & Shang, G.-F. (2021). Soil moisture retrieval from remote sensing measurements: Current knowledge and directions for the future. *Earth-Science Reviews*, *218*, 103673. doi: 10.1016/j.earscirev.2021.103673

Liu, D. L., Teng, J., Ji, F., Anwar, M. R., Feng, P., Wang, B., ... Waters, C. (2021). Characterizing spatiotemporal rainfall changes in 1960–2019 for continental australia. *International Journal of Climatology*, *41*(S1), E2420-E2444. doi: 10.1002/joc.6855

Liu, M., Hamilton, S. H., Jakeman, A. J., Lerat, J., Savage, C., & Croke, B. F. W. (2024). Assessing the contribution of hydrologic and climatic factors on vegetation condition changes in semi-arid wetlands: An analysis for the Narran Lakes. *Ecological Modelling*, *487*, 110568. doi: 10.1016/j.ecolmodel.2023.110568

Liu, X., Hu, H., & Hu, P. (2015). Accuracy Assessment of LiDAR-Derived Digital Elevation Models Based on Approximation Theory. *Remote Sensing*, *7*(6), 7062–7079. doi: 10.3390/rs70607062

Liu, Y., Wang, X., Kong, X., Ye, Y., Xu, X., Zhao, B., ... Wen, Q. (2026). Machine learning–based flood inundation mapping using fused optical and SAR remote sensing: a case study of the Miyun flood. *Frontiers in Earth Science*, *14*, 1805240. doi: 10.3389/feart.2026.1805240

Lynch, A. J., Cooke, S. J., Arthington, A. H., Baigun, C., Bossenbroek, L., Dickens, C., ... Jähnig, S. C. (2023). People need freshwater biodiversity. *WIREs Water*, *10*(3), e1633. doi: 10.1002/wat2.1633

Ma, S., Zhou, Y., Gowda, P. H., Dong, J., Zhang, G., Kakani, V. G., ... Jiang, W. (2019). Application of the water-related spectral reflectance indices: A review. *Ecological Indicators*, *98*, 68–79. doi: 10.1016/j.ecolind.2018.10.049

Madani, K. (2026). *Global Water Bankruptcy: Living Beyond Our Hydrological Means in the Post Crisis Era.* Retrieved from `https://unu.edu/inweh/collection/global-water-bankruptcy` doi: 10.53328/INR26KAM001

Makungu, E., & Hughes, D. A. (2021). Understanding and modelling the effects of wetland on the hydrology and water resources of large African river basins. *Journal of Hydrology*, *603*, 127039. doi: 10.1016/j.jhydrol.2021.127039

Marshall, V. (2017). *Overturning aqua nullius: Securing Aboriginal water rights* (Vol. 1). Aboriginal Studies Press.

Mason, T. J., Honeysett, J., Thomas, R. F., Popovic, G. C., Hosking, T., Shelly, D. J., & Bowen, S. (2022). Monitoring vital signs: Wetland vegetation responses to hydrological resources in the macquarie marshes, australia. *Austral Ecology*, *47*(6), 1296-1314. doi: 10.1111/aec.13215

Masoumi, Z., & Tourian, M. J. (2026). Absolute validation of SWOT measurements over small reservoirs using legacy photogrammetric DEMs: A case study in Zanjan Province, Iran. *Journal of Hydrology: Regional Studies*, *64*, 103229. doi: 10.1016/j.ejrh.2026.103229

Matta, G., Pant, G., Kumar, P., & Pal, R. (2026). Navigating Water Scarcity for Global Climate Change and Ramifications. *World Water Policy*, *12*(1), e70055. doi: 10.1002/wwp2.70055

Maubant, L., Dodd, L., & Tregoning, P. (2025, November). Assessing the accuracy of SWOT measurements of water bodies in Australia. *Geophysical Research Letters*, *52*. doi: 10.1029/2024GL114084

McFeeters, S. K. (1996). The use of the normalized difference water index (NDWI) in the delineation of open water features. *International Journal of Remote Sensing*, *17*(7), 1425–1432. doi: 10.1080/01431169608948714

McQuillan, K. A., Allen, G. H., Fayne, J., Gao, H., & Wang, J. (2025). Estimating wind direction and wind speed over lakes with Surface Water Ocean Topography and Sentinel-1 satellite observations. *Earth and Space Science*, *12*(3), e2024EA003971. doi: 10.1029/2024EA003971

Mitchell, A. L., Milne, A. K., & Tapley, I. (2015). Towards an operational SAR monitoring system for monitoring environmental flows in the Macquarie Marshes. *Wetlands Ecology and Management*, *23*(1), 61–77. doi: 10.1007/s11273-014-9358-2

Miura, Y., Shamsudduha, M., Suppasri, A., & Sano, D. (2025). A Global Multi-Sensor Dataset of Surface Water Indices from Landsat-8 and Sentinel-2 Satellite Measurements. *Scientific Data*, *12*(1), 1253. doi: 10.1038/s41597-025-05562-z

Mueller, N., Lewis, A., Roberts, D., Ring, S., Melrose, R., Sixsmith, J., ... Ip, A. (2016). Water observations from space: Mapping surface water from 25 years of Landsat imagery across Australia. *Remote Sensing of Environment*, *174*, 341–352. doi: 10.1016/j.rse.2015.11.003

Musa, Z. N., Popescu, I., & Mynett, A. (2015). A review of applications of satellite SAR, optical, altimetry and DEM data for surface water modelling, mapping and parameter estimation. *Hydrology and Earth System Sciences*, *19*(9), 3755–3769. doi: 10.5194/hess-19-3755-2015

Nagaraj, R., & Kumar, L. S. (2024). Extraction of Surface Water Bodies using Optical Remote Sensing Images: A Review. *Earth Science Informatics*, *17*(2), 893–956. doi: 10.1007/s12145-023-01196-0

Normandin, C., Frappart, F., Moisy, C., Baghdadi, N., Ygorra, B., Bourrel, L., ... Wigneron, J. (2026). To Which Extent the Surface Water Ocean Topography (SWOT) Mission Is Currently Able to Monitor Water Surface Elevation and Extent on the French Lakes? *Earth and Space Science*, *13*(6), e2025EA004655. doi: 10.1029/2025EA004655

Ouma, Y. O., & Tateishi, R. (2006). A water index for rapid mapping of shoreline changes of five East African Rift Valley lakes: an empirical analysis using Landsat TM and ETM+ data. *International Journal of Remote Sensing*, *27*(15), 3153–3181. doi: 10.1080/01431160500309934

Ozesmi, S. L., & Bauer, M. E. (2002). Satellite remote sensing of wetlands. *Wetlands Ecology and Management*, *10*(5), 381–402. doi: 10.1023/A:1020908432489

O'Grady, D., Leblanc, M., & Gillieson, D. (2013). Relationship of local incidence angle with satellite radar backscatter for different surface conditions. *International Journal of Applied Earth Observation and Geoinformation*, *24*, 42–53. doi: 10.1016/j.jag.2013.02.005

Pekel, J. F., Cottam, A., Gorelick, N., & Belward, A. S. (2016). High-resolution mapping of global surface water and its long-term changes. *Nature*, *540*(7633), 418-422. doi: 10.1038/nature20584

Penton, D., Marvanek, S., Mirza, F., Ticehurst, C., Sengupta, A., Teng, J., & Austin, J. (2025). *River Bathymetry in the Murray Darling Basin, Australia.* Retrieved 2026-09-21, from `https://publications.csiro.au/publications/publication/PIcsiro:EP2024-6449` doi: 10.25919/78X3-6112

Penton, D., Teng, J., Ticehurst, C., Marvanek, S., Freebairn, A., Mateo, C., ... Pollino, C. (2023). The floodplain inundation history of the Murray-Darling Basin through two-monthly maximum water depth maps. *Scientific Data*, *10*(1), 652. doi: 10.1038/s41597-023-02559-4

Platt, S., & Corrick, A. (1994). *Management of shallow freshwater wetlands for wildlife.* State of Victoria, Department of Natural Resources and Environment. Retrieved 2026-08-03, from `https://www.swifft.net.au/resources/28_management%20of%20shallow%20fresshwater%20wetlands.pdf`

Psomiadis, E., Soulis, K. X., Zoka, M., & Dercas, N. (2019). Synergistic Approach of Remote Sensing and GIS Techniques for Flash-Flood Monitoring and Damage Assessment in Thessaly Plain Area, Greece. *Water*, *11*(3). doi: 10.3390/w11030448

Rai, A. K., Cohen, T. J., Armon, M., & Marx, S. K. (2026a). SWOT satellite assessment for monitoring the extreme 2025 floods in Australia's inland Channel Country. *Environmental Research Letters*, *21*(6), 064013. doi: 10.1088/1748-9326/ae530f

Rai, A. K., Cohen, T. J., Armon, M., & Marx, S. K. (2026b). Volumetric analysis of a playa lake using SWOT data: An improved understanding of the inflows to Kati Thanda-Lake Eyre. *Journal of Hydrology*, *676*, 135652. doi: 10.1016/j.jhydrol.2026.135652

Raulings, E. J., Morris, K., Roache, M. C., & Boon, P. I. (2010). The importance of water regimes operating at small spatial scales for the diversity and structure of wetland vegetation. *Freshwater Biology*, *55*(3), 701–715. doi: 10.1111/j.1365-2427.2009.02311.x

Rayburg, S., & Thoms, M. (2009). A coupled hydraulic–hydrologic modelling approach to deriving a water balance model for a complex floodplain wetland system. *Hydrology Research*, *40*(4), 364–379. doi: 10.2166/nh.2009.110

Reid, A. J., Carlson, A. K., Creed, I. F., Eliason, E. J., Gell, P. A., Johnson, P. T. J., ... Cooke, S. J. (2019). Emerging threats and persistent conservation challenges for freshwater biodiversity. *Biological Review*, *94*(3), 849-873. doi: 10.1111/brv.12480

Ritchie, J. C. (1996). Remote sensing applications to hydrology: airborne laser altimeters. *Hydrological Sciences Journal*, *41*(4), 625–636. doi: 10.1080/02626669609491529

Robertson, H., Fennessy, S., Hilton, G., Job, N., Kumar, R., Simpson, M., ... van 't Hoff, V. (2025). *Global Wetland Outlook: Valuing, conserving, restoring and financing wetlands* (Report). Secretariat of the Convention on Wetlands. doi: 10.69556/GWO-2025-eng

Rogers, K. (2011). *Floodplain Wetland Biota in the Murray-Darling Basin: Water and Habitat Requirements*. CSIRO Publishing. doi: 10.1071/9780643100992

Salameh, E., Sengsourinho, L., Normandin, C., Sollier, V., & Frappart, F. (2026). Assessing SWOT capabilities for monitoring floodplain water dynamics in the Paraná Basin. *Scientific Reports*, *16*(1), 22906. doi: 10.1038/s41598-026-53807-7

Sales, L., Beltrão, D., Lappicy, T., Jesus, L., Almeida, T., & Cicerelli, R. (2025). Mapping of wetlands in the Pantanal with SWOT. In *2025 Latin American GRSS ISPRS Remote Sensing Conference (LAGIRS)* (pp. 1–7). IEEE. doi: 10.1109/LAGIRS68367.2025.11414789

Sayer, C. A., Fernando, E., Jimenez, R. R., Macfarlane, N. B. W., Rapacciuolo, G., Böhm, M., ... Darwall, W. R. T. (2025). One-quarter of freshwater fauna threatened with extinction. *Nature*, *638*(8049), 138–145. doi: 10.1038/s41586-024-08375-z

Shan, J., & Toth, C. (Eds.). (2008). *Topographic Laser Ranging and Scanning: Principles and Processing.* CRC Press. doi: 10.1201/9781420051438

Shi, T., & Xu, H. (2019). Derivation of Tasseled Cap Transformation Coefficients for Sentinel-2 MSI At-Sensor Reflectance Data. *IEEE Journal of Selected Topics in Applied Earth Observations and Remote Sensing*, *12*(10), 4038–4048. doi: 10.1109/JSTARS.2019.2938388

Shirafkan, S., Sharifi, M. A., & Tourian, M. J. (2026). Improving water pixel detection in SWOT Pixel Cloud(PIXC) data over small reservoirs using machine learning methods. *Journal of Hydrology*, *679*, 136247. doi: 10.1016/j.jhydrol.2026.136247

Shook, K., Spiteri, R., Pomeroy, J., Liu, T., & Sharomi, O. (2021). WDPM: the Wetland DEM Ponding Model. *Journal of Open Source Software*, *6*, 2276. doi: 10.21105/joss.02276

Sims, N., Warren, G., Overton, I., Austin, J., Gallant, J., King, D., ... Cuddy, S. (2014). *RiM-FIM floodplain inundation modelling for the Edward-Wakool, Lower Murrumbidgee and Lower Darling River systems.* CSIRO. doi: 10.4225/08/584D978E3E0C1

Slagter, B., Tsendbazar, N.-E., Vollrath, A., & Reiche, J. (2020). Mapping wetland characteristics using temporally dense Sentinel-1 and Sentinel-2 data: A case study in the St. Lucia wetlands, South Africa. *International Journal of Applied Earth Observation and Geoinformation*, *86*, 102009. doi: 10.1016/j.jag.2019.102009

Smart, J. C. R., Harte, J., Cook, M., Hasan, S., Castley, J. G., & Teixeira, A. L. d. F. (2026). An interdisciplinary analysis of recreational birdwatching and wetland extent in the Murray-Darling Basin, Australia. *iScience*, *29*(2), 114743. doi: 10.1016/j.isci.2026.114743

Spatial Services, NSW Government. (2025). *Grawin LiDAR Elevation Data.* Retrieved from `https://elevation.fsdf.org.au/`

State of Queensland Department of Natural Resources, Mines and Energy. (2019). *Queensland LiDAR Data - Lower Balonne 2018 Project.* Retrieved from `https://elevation.fsdf.org.au/`

Streever, W. J., Callaghan-Perry, M., Searles, A., Stevens, T., & Svoboda, P. (1998). Public attitudes and values for wetland conservation in New South Wales, Australia. *Journal of Environmental Management*, *54*(1), 1–14. doi: 10.1006/jema.1998.0224

Sudriani, Y., Sebestyén, V., & Abonyi, J. (2023). Surface Water Monitoring Systems—The Importance of Integrating Information Sources for Sustainable Watershed Management. *IEEE Access*, *11*, 36421–36451. doi: 10.1109/ACCESS.2023.3263802

Sun, W., Wei, Z., Sun, H., & He, H. (2022). Review on the Application of Airborne LiDAR in Active Tectonics of China: Dushanzi Reverse Fault in the Northern Tian Shan. *Frontiers in Earth Science*, *10*. doi: 10.3389/feart.2022.895758

Surface Water Ocean Topography (SWOT). (2025). *SWOT Level 2 Water Mask Pixel Cloud Data Product, Version D. Ver. D. PO.DAAC.* (Dataset accessed 2026-05-04 at https://doi.org/10.5067/SWOT-PIXC-D)

SWOT-IS-CDM-1447-CNES, Revision B. (2024). *SWOT Auxiliary Data Description Document: Prior Water Mask (WaterMask)* (Tech. Rep.). Centre National d'Etudes Spatiales.

Taib, M., & Tregoning, P. (2026a). *Constraints on the accuracy of swot water detection in wetlands.* Zenodo. Retrieved from `https://doi.org/10.5281/zenodo.22324561`

Taib, M., & Tregoning, P. (2026b). Constraints on the accuracy of SWOT water detection in wetlands. *Geophysical Research Letters*. (Manuscript under review.)

Teng, J., Jakeman, A. J., Vaze, J., Croke, B. F. W., Dutta, D., & Kim, S. (2017). Flood inundation modelling: A review of methods, recent advances and uncertainty analysis. *Environmental Modelling & Software*, *90*, 201–216. doi: 10.1016/j.envsoft.2017.01.006

Teng, J., Penton, D., Ticehurst, C., Sengupta, A., Freebairn, A., Marvanek, S., ... Morton, S. (2022). A Comprehensive Assessment of Floodwater Depth Estimation Models in Semiarid Regions. *Water Resources Research*, *58*(11), e2022WR032031. doi: 10.1029/2022WR032031

Thoms, M., Capon, S., James, C., Padgham, M., & Rayburg, S. (2007). *The Narran Ecosystem Project: the response of a terminal wetland system to variable wetting and drying. Final report to the Murray-Darling Basin Commission.* Retrieved 2025-10-09, from `https://www.researchgate.net/doi/10.13140/2.1.2194.6564`

Ticehurst, C., Joshi, R., Hussain, S., Walker, S., Opie, K., & Donohue, R. (2025). *Annual vegetation height for Australia for 2019 to 2024.* CSIRO. Retrieved 2026-07-15, from `https://data.csiro.au/collection/csiro:3A66385v1` doi: 10.25919/KE8A-VT79

Ticehurst, C., & Newnham, G. (2024). Producing annual australia-wide vegetation height images from GEDI and Landsat data. *International Journal of Remote Sensing*, *45*(18), 6445–6469. doi: 10.1080/01431161.2024.2391093

Ticehurst, C., Teng, J., & Sengupta, A. (2022). Development of a Multi-Index Method Based on Landsat Reflectance Data to Map Open Water in a Complex Environment. *Remote Sensing*, *14*(5). doi: 10.3390/rs14051158

Townsend, P. A., & Walsh, S. J. (1998). Modeling floodplain inundation using an integrated GIS with radar and optical remote sensing. *Geomorphology*, *21*(3), 295–312. doi: 10.1016/S0169-555X(97)00069-X

Usman, M., Chua, L. H. C., Irvine, K. N., & Teang, L. (2025). Estimating water surface elevation for a wetland using integrated multi-sourced remote sensing data. *Wetlands Ecology and Management*, *33*(1), 20. doi: 10.1007/s11273-025-10032-9

Van Dijk, A. I. J. M., & Renzullo, L. J. (2011). Water resource monitoring systems and the role of satellite observations. *Hydrology and Earth System Sciences*, *15*(1), 39–55. doi: 10.5194/hess-15-39-2011

Vinci, G., Vanzani, F., Fontana, A., & Campana, S. (2025). LiDAR Applications in Archaeology: A Systematic Review. *Archaeological Prospection*, *32*(1), 81–101. doi: 10.1002/arp.1931

Wechsler, S. (2007). Uncertainties associated with digital elevation models for hydrologic applications: A review. *Hydrology and Earth System Sciences*, *11*. doi: 10.5194/hess-11-1481-2007

Wu, Q., & Lane, C. R. (2017). Delineating wetland catchments and modeling hydrologic connectivity using lidar data and aerial imagery. *Hydrology and earth system sciences*, *21*(7), 3579–3595. doi: 10.5194/hess-21-3579-2017

Xu, H. (2006). Modification of normalised difference water index (NDWI) to enhance open water features in remotely sensed imagery. *International Journal of Remote Sensing*, *27*(14), 3025–3033. doi: 10.1080/01431160600589179

Yan, W. Y., Shaker, A., & El-Ashmawy, N. (2015). Urban land cover classification using airborne LiDAR data: A review. *Remote Sensing of Environment*, *158*, 295–310. doi: 10.1016/j.rse.2014.11.001

Zhao, C., Wei, H., Feyisa, G. L., De Castro Tayer, T., Ma, G., Wu, H., & Pan, Y. (2025). Evaluating spectral indices for water extraction: Limitations and contextual usage recommendations. *International Journal of Applied Earth Observation and Geoinformation*, *139*, 104510. doi: 10.1016/j.jag.2025.104510